Journal of Medicinal Chemistry

Article

pubs.acs.org/jmc

Fragment Growing and Linking Lead to Novel Nanomolar Lactate Dehydrogenase Inhibitors

Anna Kohlmann,* Stephan G. Zech, Feng Li, Tianjun Zhou, Rachel M. Squillace, Lois Commodore, Matthew T. Greenfield, Xiaohui Lu,† David P. Miller, Wei-Sheng Huang, Jiwei Qi, R. Mathew Thomas, Yihan Wang, Sen Zhang, Rory Dodd, Shuangying Liu, Rongsong Xu, Yongjin Xu, Juan J. Miret,‡ Victor Rivera, Tim Clackson, William C. Shakespeare, Xiaotian Zhu, and David C. Dalgarno

ARIAD Pharmaceuticals, Inc., 26 Landsdowne Street, Cambridge, Massachusetts 02139, United States

Supporting Information

ABSTRACT: Lactate dehydrogenase A (LDH-A) catalyzes the interconversion of lactate and pyruvate in the glycolysis pathway. Cancer cells rely heavily on glycolysis instead of oxidative phosphorylation to generate ATP, a phenomenon known as the Warburg effect. The inhibition of LDH-A by small molecules is therefore of interest for potential cancer treatments. We describe the identification and optimization of LDH-A inhibitors by fragment-based drug discovery. We applied ligand based NMR screening to identify low affinity fragments binding to LDH-A. The dissociation constants (K_d) and enzyme inhibition (IC_{50}) of fragment hits were measured by surface plasmon resonance (SPR) and enzyme assays, respectively. The binding modes of selected fragments were investigated by X-ray crystallography. Fragment growing and linking, followed by chemical optimization, resulted in nanomolar LDH-A inhibitors that demonstrated stoichiometric binding to LDH-A. Selected molecules inhibited lactate production in cells, suggesting target-specific inhibition in cancer cell lines.

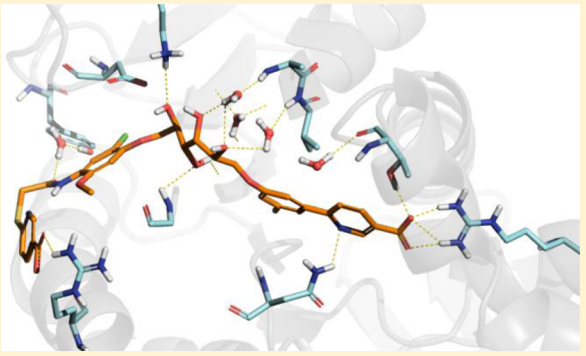

INTRODUCTION

Otto Warburg's historic discovery showing that cancer cells preferentially derive ATP through glycolysis rather than oxidative phosphorylation provided the first tangible connection between energy metabolism and cancer.[1] Despite the low efficiency of generating ATP from glucose by utilizing glycolysis rather than oxidative phosphorylation, the increased rate of glycolysis in cancer cells is believed to ensure rapid generation of energy and biomass needed for cellular proliferation.[2−4] Dependence on glycolysis may also provide an advantage for cancer cells to survive and grow under hypoxic conditions that characterize the environment of solid tumor. Altered cancer cell energy metabolism has been categorized as an emerging hallmark of cancer,[5,6] and thus, inhibition of metabolic processes associated with cancer cell growth constitutes a promising approach in the search for new cancer therapies.

One molecular target in the glycolytic pathway is the enzyme lactate dehydrogenase (LDH) which catalyzes the interconversion of lactate and pyruvate as the last step of glycolysis. In mammalian cells, there are two LDH isoforms, LDH-A and LDH-B, with the A form having higher intrinsic activity to catalyze pyruvate transformation to lactate.[7,8] LDH exists in tetramer form in human cells, comprising combinations of the A and B isoforms. Specifically, LDH-5, composed of four LDH-A monomers, is mostly expressed in liver and muscle and favors the conversion of pyruvate to lactate.[9]

Several lines of evidence suggest that LDH-A plays a critical role in cancer cell proliferation. Up-regulation of LDH-A mRNA and protein expression have been reported across numerous cancer types.[10−15] Regulation of the LDH-A gene and other genes involved in promoting glycolysis is under control of potentially oncogenic transcription factors such as c-Myc and HIF-1α.[16−19] Aberrant activation of these oncogenes results in elevated uptake of glucose and increased production of lactate. Reduction of LDH-A by expression of targeted siRNA in cancer lines produces inhibition of cell growth under hypoxic conditions and dramatically reduces tumor formation in mouse models.[14,15] Knockdown of LDH-A also increases oxygen consumption, stimulates mitochondrial respiration, and induces oxidative stress while adding back LDH-A protein reverses these phenotypes.[20,21] Finally, a potential safety concern of inhibiting LDH-A for cancer treatment is addressed by the observation that individuals who naturally lack LDH-A do not show any symptoms under normal conditions except some degree of muscle rigidity and myoglobinuria after intense exercise.[22] Therefore, LDH-A is a potentially important and relatively safe metabolic target for inhibition of the highly activated glycolysis pathway in cancer cells.

LDH-A is a highly conserved protein that contains approximately 330 amino acids in a bilobal structure.[9] Although the

Received: October 12, 2012

dx.doi.org/10.1021/jm3014844 | J. Med. Chem. XXXX, XXX, XXX−XXX

LDH enzyme exists as a tetramer, each LDH-A monomer independently possesses full catalytic function. The large domain adopts a Rossmann fold[23] and forms the NADH cofactor binding site, while the small domain, with a mixed α/β structure, constitutes the substrate binding domain. Mechanistic studies have revealed an ordered sequence of cofactor and substrate binding events in LDH-A.[24,25] The cofactor NADH binds first and prepares the binding site for the substrate binding, which is followed by the closure of the catalytic loop (residues 98−107), bringing the catalytic Arg105 into contact with substrate, followed by hydride transfer. The crystal structure of human LDH-A containing both NADH and the LDH inhibitor oxamate,[9] a pyruvate mimic, shows that NADH binds to LDH-A in an extended conformation with the nicotinamide and adenosine portions of NADH occupying the two ends of the cofactor active site separated by a distance of approximately 20 Å.[9] The substrate analogue oxamate binds parallel to the nicotinamide while forming a bifurcated hydrogen bond to the guanidine group of Arg168 of LDH-A, and hydrogen bonds to catalytic residues His192 and Arg105. Both the NADH and pyruvate substrate binding sites present potential opportunities for developing small molecule LDH-A inhibitors. However, the polar nature of the active site, small size of the substrate site, and the large distance between the adenine and nicotinamide sites pose a challenge to the discovery of potent small molecule inhibitors.

Although LDH-A is well characterized, only a few LDH-A inhibitors are reported in the literature. Most published LDH-A inhibitors have relatively poor inhibitory activities with low μM IC_{50} in enzymatic assays. Among them, oxamate, a pyruvate substrate analogue, has been shown to have $K_i \approx 26$ μM against LDH-A.[9] Several chemical series were designed and synthesized based on oxamate.[26,27] These compounds have high molecular weight and diverse functional groups; however, they exhibit relatively poor inhibitory activities. In addition to the oxamate analogues, a natural product named gossypol and the gossypol analogue FX11 were reported as LDH-A inhibitors with K_i values in the low micromolar range.[20] Recently a new chemical series of *N*-hydroxyindole-based LDH-A inhibitors was published with reported enzymatic inhibitory activity in the low micromolar range.[28] Finally, a recent publication by Ward et al. described fragment-based discovery of LDH-A inhibitors.[29] This study was published as our research program was concluded. The authors report a similar fragment-linking workflow described here; interestingly both groups achieved nanomolar potency with chemically different linked structures.

In search of novel LDH-A inhibitors, we took a fragment-based approach to identify low molecular weight chemical compounds that bind to LDH-A. As illustrated in Figure 1, we also performed a virtual screen of commercially available compounds from the ZINC[30] database on LDH-A, in parallel to our fragment based efforts. Although several virtual screening hits showed activity in the enzyme assay (300−800 μM), the activity was not confirmed by our secondary screens. The hits displayed aggregator properties and were not followed up for optimization.

In the search of small, specific fragments, a chemically diverse, rule-of-three (Ro3)[31] compliant fragment library was screened in the LDH-A binding assay monitored by saturation transfer difference NMR (STD-NMR)[32] and followed by surface plasmon resonance (SPR)[33] K_d measurement experiments. Crystal structures of the identified fragment hits bound in LDH-A were determined, and the structural information was used to guide fragment evolution and optimization. These fragment-based efforts led to the identification of novel LDH-A inhibitors bound

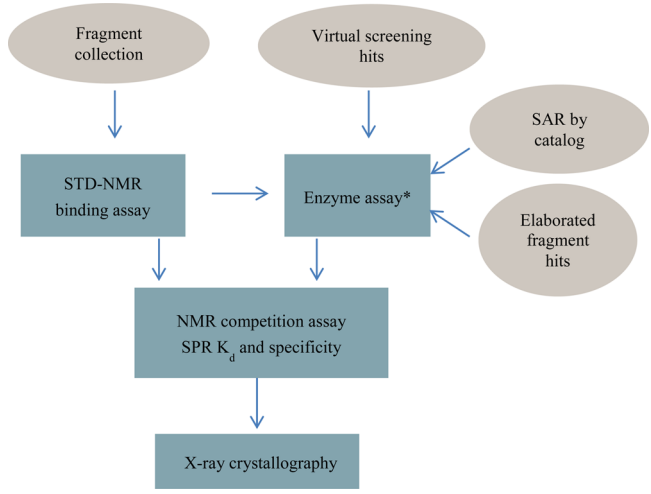

Figure 1. Fragment based drug discovery workflow employs multiple confirmatory assays. The asterisk (*) indicates that enzyme assays are run in the presence of detergent to rule out aggregation.

in two subpockets of the LDH-A catalytic active site. Then a linking strategy was deployed to improve the inhibitory activities and led to the identification of a novel chemical series that inhibits LDH-A with IC_{50} in the nanomolar range in the enzyme assay. Some of the compounds demonstrated inhibition of lactate production in cellular assays, suggesting that they inhibit the LDH-A target in cancer cell lines.

RESULTS AND DISCUSSION

Structural Analysis. To investigate the binding site, we solved the X-ray crystal structure of rabbit LDH-A in complex with NADH and oxamate and the structure of rabbit LDH-A in complex with AMP. The rabbit LDH-A has 93% sequence similarity to human LDH-A[34] and was the optimal system for obtaining well-diffracting cocrystals with AMP. The LDH-A/AMP system was required for soaking the fragments, as discussed below. The structures exhibit a similar fold to the human LDH-A/NADH/oxamate ternary structure that was previously reported (PDB code 1i10[9]). However, in our structures, the active site loop (residues 98−110) remained disordered. To map binding site properties in LDH-A, we applied SiteMap[35,36] and WaterMap.[37] SiteMap highlighted the largely hydrophilic nature of the binding cavity, with hydrophobic patches at the nicotinamide and the adenosine sites that are far removed from each other. Analysis of the hydration sites generated by WaterMap confirmed this finding, with high-energy water located in the adenosine binding pocket, the nicotinamide site, and the substrate site. The computational investigation of LDH-A indicated the presence of a large, hydrophilic site of challenging druggability. The buried energetic hot spots are far apart, indicating that a linking strategy connecting two sites might be necessary to achieve optimal potency against LDH-A.

Fragment Screening. To identify novel fragments binding to LDH-A, we used NMR spectroscopy as the primary screening method to detect and validate protein−ligand interaction. A library of 735 diverse Ro3 compliant small molecules (Maybridge) was investigated using STD-NMR experiments. As shown previously,[32] this magnetization transfer method is well suited to identify weakly binding fragments with affinities ranging from tens of micromolar to millimolar K_d.

The NMR screen returned a total of 38 hits (5.2% hit rate), 19 of which were carboxylic acids. The high hit rate for carboxylic

dx.doi.org/10.1021/jm3014844 | J. Med. Chem. XXXX, XXX, XXX−XXX

acids (~50% of hits compared to 16% of total compounds in the library) implies a preference for small, negatively charged molecules in the binding site, potentially mimicking the pyruvate binding pattern. Similar findings have been previously reported.[38,39] NMR competition binding experiments with the natural cofactor NADH were performed in order to (i) further validate the hits, (ii) confirm the site of binding, and (iii) distinguish between specific and unspecific binding of fragments.

As an example, Figure 2 shows the reference NMR spectrum of fragment **1** in the presence of LDH-A (panel A) along with the

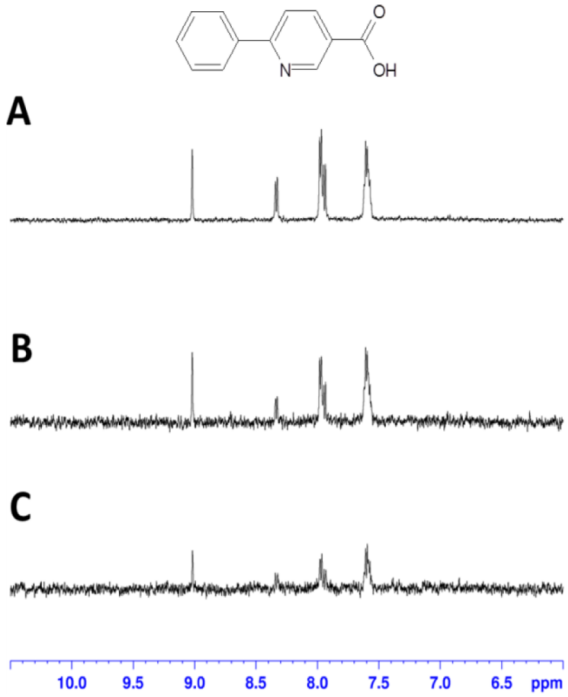

Figure 2. (A) Structure of compound **1** and reference NMR spectrum. (B) STD-NMR spectrum of **1** in the presence of 20 μM rabbit LDH-A. (C) STD-NMR spectrum of **1** in the presence of 20 μM rabbit LDH-A and 250 μM NADH. All spectra were obtained at 2 mM **1**. Addition of NADH results in a reduction of STD signal intensity by about 50%, indicating competition between NADH and compound **1**.

STD-NMR spectrum in panel B. Upon addition of NADH (panel C), the intensity of STD signals of compound **1** is reduced by a factor of 2, demonstrating NADH competitiveness. The remaining STD-NMR signal of **1** in the presence of NADH can be explained by (i) incomplete saturation of the NADH binding site due to its limited potency ($K_M \approx 10$ μM) or (ii) alternative binding sites for compound **1** including unspecific binding at the protein surface. However, a reduction of STD signal of about 50% or more in the presence of NADH was sufficient to confirm compounds binding to the substrate/cofactor sites for the majority of early fragment hits. The competition of most fragments with NADH is consistent with the observation of a very low hit rate in an NMR screen run in the presence of NADH. Apparently, most fragments in our library were too large to fit into the small substrate binding site in the presence of NADH or were not potent enough to displace NADH.

Unfortunately, even though binding to the substrate/cofactor site was demonstrated by NMR competition experiments, most of the initial fragments did not show significant inhibition of the enzyme reaction ($IC_{50} > 1$ mM), making it difficult to follow SAR for early hits using enzyme assays, and necessitated implementation of orthogonal biophysical techniques, such as SPR.

Investigation of the initial fragment hits by SPR revealed only weak interaction with LDH-A, with K_d values ranging between 1 and 5 mM for most compounds. To obtain guidance on chemical optimization of the fragments, crystals of LDH-A with AMP, back-soaked to remove AMP, were utilized for soaking the fragment hits and subsequent crystallography. Clear electron density was visible for one of the soaked compounds (fragment 1, Figure 3). An unambiguous binding mode was observed. The

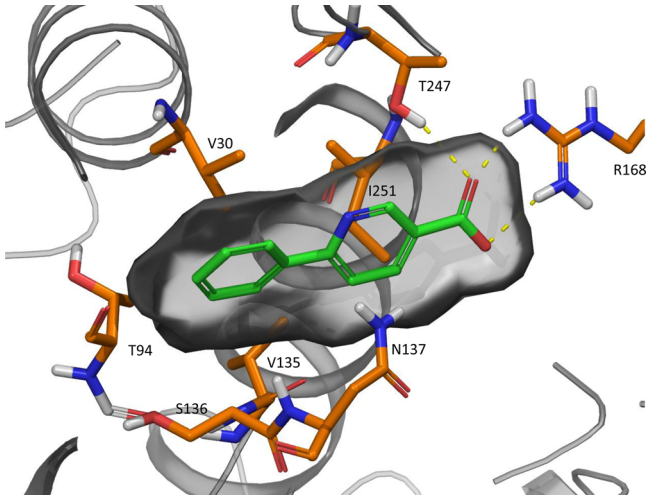

Figure 3. Binding of fragment **1** in the active site of LDH-A.

fragment occupies the oxamate and part of the nicotinamide binding sites, with the carboxylic acid making a salt bridge to the catalytic residue Arg168. An additional hydrogen bond is formed between one of the carboxylic oxygen atoms and the hydroxyl group of the catalytic Thr247. The pyridine ring is in contact with the hydrophobic side chains of Ile251 and Val30 and has additional favorable interactions with Asn137. The phenyl ring makes productive interactions with Val30, Val135, Thr94, and Ser136. Superposition of the X-ray crystal structure with that of the LDH-A ternary complex (1i10) shows that the fragment extends in the direction of the pyrophosphate group of NADH, with the phenyl ring occupying the position of the sugar moiety. Although fragment **1** was inactive in the enzyme assay ($IC_{50} > 2$ mM), a K_d of 2.3 mM was detected in the SPR assay.

Fragment **1** was selected as the starting point for exploration because of the ease of synthetic modification and the availability of a crystal structure to guide the optimization. After analyzing available vectors for fragment growing, we modified the fragment at the para position of the phenyl ring (C4) to access the open cofactor-binding pocket. Meta-substitutions on the phenyl ring (positions C3 and C5) were also explored to engage protein interactions. Specifically, a small hydrophobic pocket was observed in the crystal structure, formed between two strands at the ends of the β sheets by residues Ser136, Val135, and Thr94. Introduction of fluorine at position C5 to fill that pocket improved activity. At position C3, hydrophilic chains were added to facilitate hydrogen bonding interactions with the main chain of the protein. Although C4-substitutions yielded no improvement in IC_{50}, combining modifications at positions C5 and C3 yielded compounds with measurable IC_{50} in the low millimolar range (for example, see compounds **2** and **3** in Table 1). Finally, we attempted fragment growing into the nicotinamide site by

dx.doi.org/10.1021/jm3014844 | J. Med. Chem. XXXX, XXX, XXX−XXX

Table 1. Structures and Activity of Selected Fragments[a]

Compound	Structure	IC_{50},μM	K_d,μM	LE
1	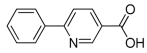	> 2000	2300	0.18
2	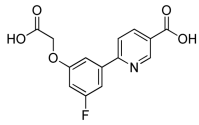	2200	1300	0.14
3	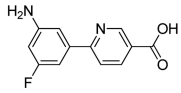	1300	na	
4	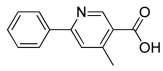	na	1900	0.17
5	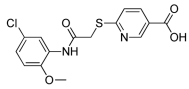	770	137	0.17
6	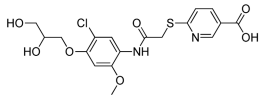	342	360	0.12

[a]LE computed as pK_d/(no. of heavy atoms).

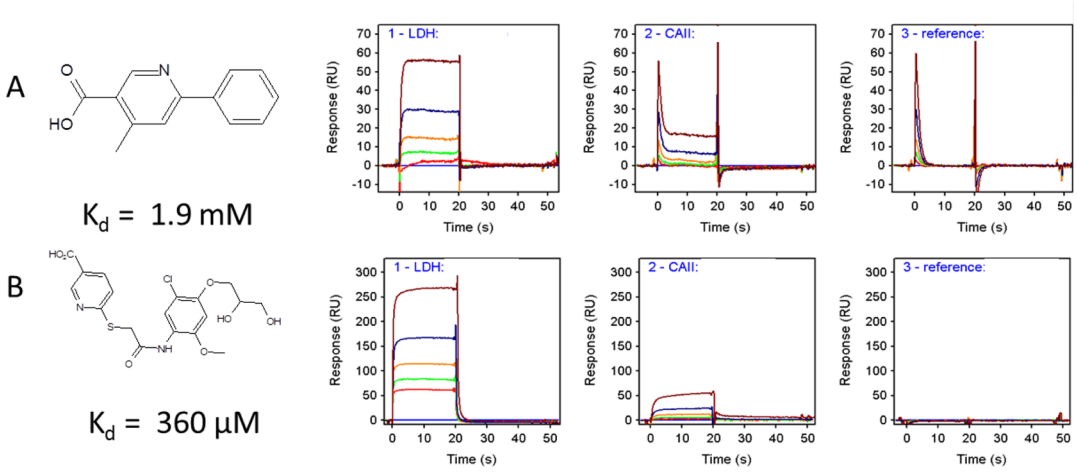

Figure 4. SPR sensograms for compound **4** (A) and compound **6** (B) binding to the surface with immobilized LDH-A (1), CA-II (2), or an empty surface (3). The sensograms were obtained at 20 °C using a 2-fold dilution series with an upper concentration of 1 mM. Compounds in the millimolar affinity range were found to have significant off-target affinity as demonstrated by the binding to CA-II. Elaborated hits, such as compound **14**, not only showed better affinity to LDHA but also improved selectivity.

introducing C3 and C4 substitutions onto the pyridine ring; however, these derivatives showed only minor affinity improvements (for example, see compound **4**, with $K_d \approx 1.8$ mM) and still displayed significant off-target effects to the SPR reference protein (Figure 4A).

Adenosine Site. In the course of screening elaborated analogues of compound **1**, compound **5** was identified (Figure 5A). With an IC_{50} of 770 μM in enzyme assay and a K_d of 137 μM measured by SPR, it was the strongest binder derived from the initial fragments thus far. However, when compound **5** was soaked in the LDH-A crystal, it bound in the adenosine site rather than in the oxamate site analogous to its parent compound **1**. In the observed binding mode, the phenyl ring occupies a lipophilic pocket normally filled by the adenosine moiety of NADH (Figure 5B). The phenyl is sandwiched between the side chains of Ile115 and Ile119 on the bottom and Val52 on the top. The 1-methoxy group is bound through van der Waals contacts to Ile115 and Phe118. The 4-Cl substituent is in contact with the backbone atoms of Asp51 and residues Gly26 and Val25. The flexible linker lies on the surface of the protein and makes favorable interactions with Ile115 and the side chains of Ile119 and Phe118. Finally, the pyridine ring interacts with Asn114 and Ile115. The carboxylic acid forms a salt bridge with the side chain of Arg111. An internal hydrogen bond between the amide nitrogen of the linker and the pyridine N stabilizes the bound conformation. Replacement or deletion of the phenyl ring substituents or linker modifications resulted mostly in reduced potency. However, we were successful in introducing substitutions at position

dx.doi.org/10.1021/jm3014844 | J. Med. Chem. XXXX, XXX, XXX−XXX

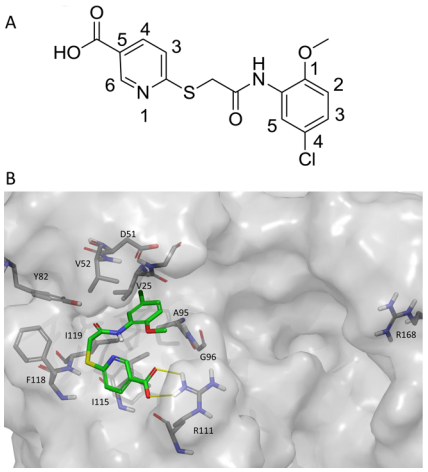

Figure 5. (A) Compound **5**. (B) The crystal structure reveals compound **5** bound in the adenosine binding site of LDH-A. Arg168 is shown for reference to indicate the oxamate binding site.

3 of the phenyl ring, with the goal of extending the molecule into the binding site of LDH-A. To mimic the interactions that the sugar moiety of NADH makes with the protein, we added an oxypropane-1,2-diol group and thereby gained some potency (compound **6**; Figure 4B; IC_{50} = 342 μM, K_d = 360 μM). An additional hydrogen bond was formed between the 3-hydroxy group of the molecule and the side chain of Asp51. This hydrogen bond is also observed in the LDH-A/NADH/oxamate structure, where the adenosine sugar interacts with the side chain of Asp51 via one of its hydroxyl groups. Further substitutions at the 1 and 4 positions of the phenyl ring, as well as in the linker, and the replacement of carboxylic acid failed to increase potency. However, adenosine site binders showed improved potency with K_d values in the 200−400 μM range and improved selectivity for LDH-A, compared to oxamate site binders. To quantify the potency improvement, we computed the ligand efficiency (LE) of the elaborated fragments. We saw either no improvement or loss of LE in the process of fragment growing (Table 1), with both initial fragment hits and elaborated fragments exhibiting fairly low LE. The difficulty in improving LE is a consequence of the low druggability of the LDH-A binding site. We therefore concluded that for significant potency gain we would need to adopt a fragment-linking approach: bridging the gap between potent oxamate and adenosine fragments with an appropriately spaced chemical linker.

Linked Compounds. Cosoaking the two molecules in the LDH-A crystal, we determined the structures of compounds **2** and **6** in the LDH-A binding site (Figure 6). The two molecules assume binding modes identical to the modes in the individual crystal structures. The distance between the terminal carbons of these compounds is 3.3 Å. Flexible linkers of seven to nine atoms were introduced to bridge the space between the two molecules. Initially, a simple ether linkage was used (compound **7**), with resulting IC_{50} of 59 μM for the linked compound. To explore functional groups and linker lengths, compounds with functional groups such as ester, amide, NH, and OH in the linker were synthesized and tested (Table 2). An eight-atom linker presented the optimal geometry for connecting the two binding sites. The most active molecule synthesized was compound **9**, with an eight-atom linker containing four hydroxyl groups. The X-ray crystal structure was solved by soaking compound **9** with LDH-A; however, a structure of an analogue compound **8** had stronger electron density (Figure 7). The interactions of

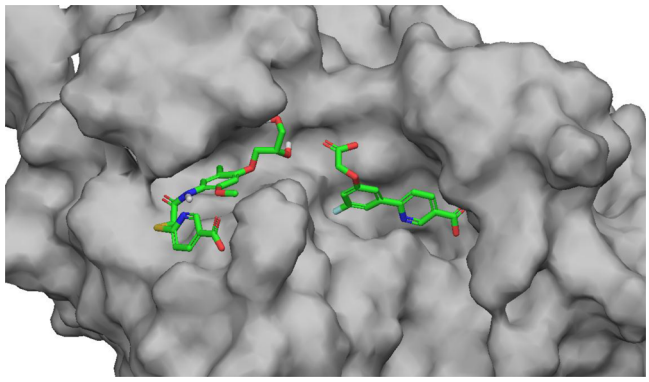

Figure 6. Cosoaked structures of compounds **2** and **6** in the active site of LDH-A. The side chain of Arg98 was removed for an unobstructed view of the binding site.

compounds **9** and **8** with the protein were similar and consistent with those described above for the cosoaked parent fragments. The eight-atom linker spanned the solvent-exposed region connecting the two binding sites, with the hydroxyl groups making direct and water-mediated hydrogen bonds to the backbone atoms of the protein. Specifically, three crystallographic water molecules were detected in the linker region. These waters form a network of hydrogen bonds, connecting 1-hydroxyl and 3-hydroxyl to the backbone nitrogen atoms of Val30, Ala29, and Gly31. One additional water molecule is wedged between the phenyl ring of the inhibitor and the backbone carbonyl atom of Thr247. The carbonyl atom of the S-containing linker in the adenosine site forms a hydrogen bond with the side chain of Tyr82, mediated by the fifth crystallographic water. Interestingly, the side chain of Arg111 in all these structures was disordered. Clearly, the exact positioning of the four hydroxyl groups was key to activity. The removal of these groups leads to a marked loss of potency, as did the modification of the stereochemistry (see compound **11**). We also explored an amide-containing linker (compound **10**) in an attempt to engage water-mediated hydrogen bonds without introducing hydroxyl groups; however, this resulted in loss of activity.

Linking of fragments in adenosine and pyruvate binding pockets yielded compounds with greatly improved potency and selectivity. Figure 8A shows the dose response curves for enzyme inhibition of compound **8** in the presence and absence of detergent. The results are reproducible within the margin of experimental error (2-fold). The SPR sensogram of compound **7** is shown in Figure 8B. The SPR response can be well fitted with a simple 1:1 binding model. Both kinetic and equilibrium K_d analysis are in agreement with an affinity of 0.9 μM in the enzyme assay for this compound. No affinity to the SPR reference surface containing immobilized carbonic anhydrase II (CA-II) was detected. Finally, the potency gain in linking compounds was achieved without a loss in LE compared to the parent fragments (Tables 1 and 2).

Finally, anticipating potential permeability issues in a cellular assay, we synthesized analogues without one or both terminal carboxylic acids (Table 3, compounds **12**, **13**, **14**). However, the removal of the carboxylic acid leads to at least a 20-fold potency loss (see compound **12** relative to reference compound **9**). The SAR highlights the importance of both salt bridges observed in the crystal structure.

Chemistry. *Compound 1.* Compound **1** was purchased from Maybridge as part of the fragment screening collection.

dx.doi.org/10.1021/jm3014844 | J. Med. Chem. XXXX, XXX, XXX−XXX

Table 2. SAR for Selected Linked Compounds[a]

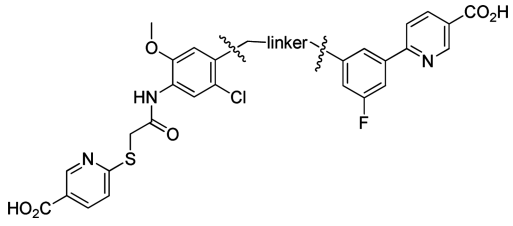

Compound	Linker	IC_{50},μM	K_d,μM	LE
7	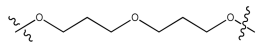	59.0	0.850	0.13
8	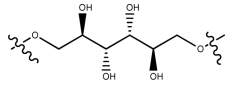	0.440	0.068	0.14
9	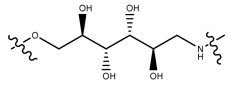	0.120	0.019	0.15
10	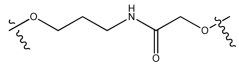	2.40	0.175	0.14
11	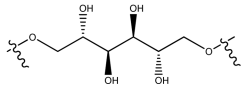	15.2	12.0	0.10

[a]LE computed as pK_d/(no. of heavy atoms).

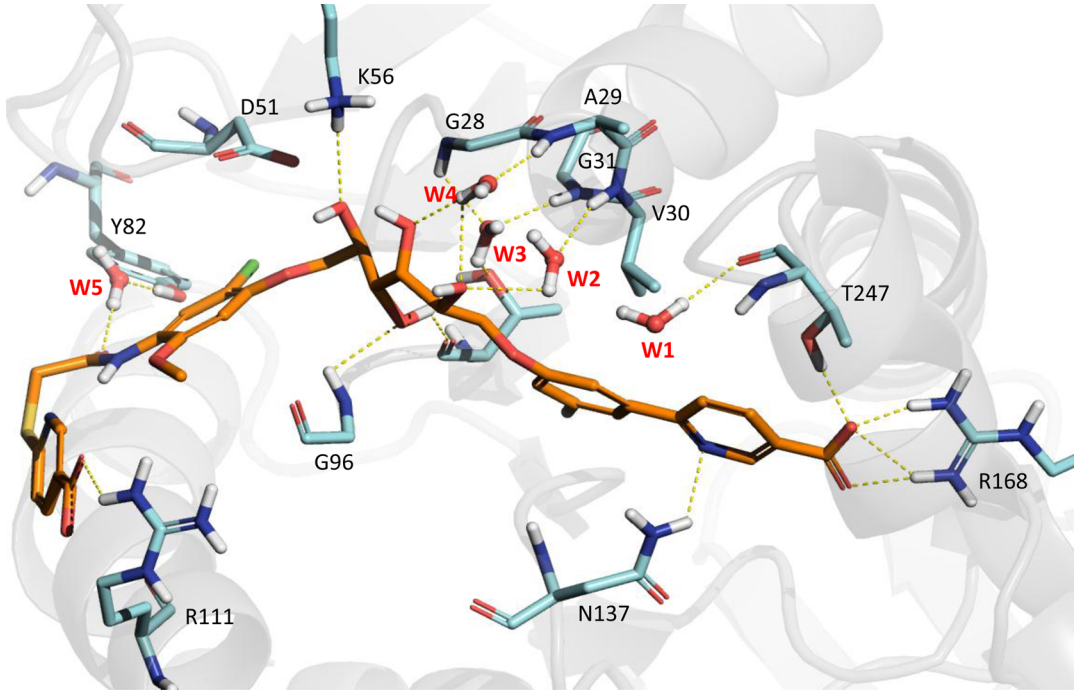

Figure 7. X-ray crystal structure of linked compound **8** in LDH-A with hydrogen bonding network shown.

Compound ***2***. Compound **2** was synthesized by a Suzuki coupling of 6-bromonicotinic acid and 3-(carboxymethoxy)-5-fluorophenylboronic acid without protection as shown in Scheme 1. HPLC purification afforded the desired product in 14% yield.

Compound ***3***. Synthesis of compound **3** proceeded via Suzuki coupling of methyl 6-chloronicotinate and 3-amino-5-fluorophenylboronic acid to give intermediate compound **15**. Hydrolysis with LiOH in MeOH/H_2O furnished the target compound **3** as depicted in Scheme 2.

dx.doi.org/10.1021/jm3014844 | J. Med. Chem. XXXX, XXX, XXX−XXX

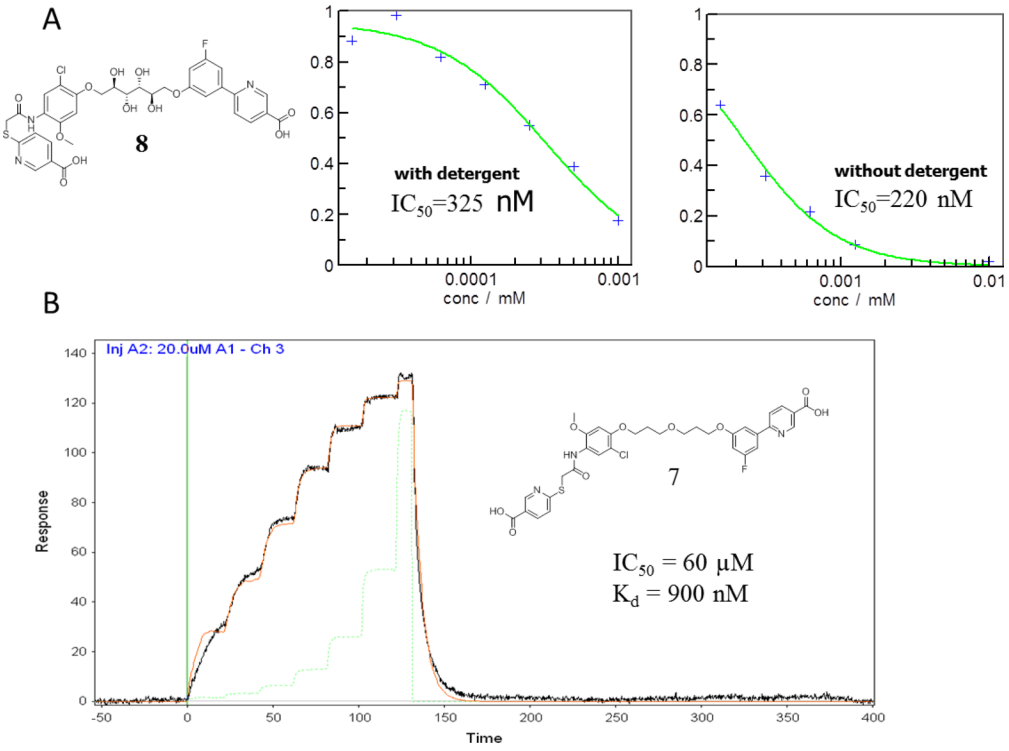

Figure 8. Biochemical and biophysical evaluation of linked compounds. (A) Compound **8** displayed enzyme inhibition virtually independent of detergent. (B) SPR sensogram (black) of compound **7** obtained with "fast-step" concentration ramping (dotted green line). The data were fitted (orange line) to a 1:1 binding model and yielded a K_d of 0.9 μM, in agreement with an IC_{50} of 60 μM.

Table 3. Modification of Lead Compound 9 To Improve Cellular Permeability

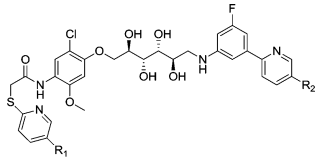

compd	R_1	R_2	IC_{50}, μM	K_d, μM
9	COOH	COOH	0.120	0.019
12	H	COOH	2.4	0.222
13	COOH	H	13	2.95
14	CO_2Me	CO_2Me	>10000	na

Compound ***4***. The synthesis of target compound **4** was initiated via esterification of 4,6-dichloronicotinic acid to afford ester **16**. Selective Suzuki coupling at the 4-position of compound **16** gave compound **17**. A subsequent Negishi reaction introduced a 6-methyl group to furnish compound **18**, which was then hydrolyzed with LiOH in EOH/H_2O to yield **4** as shown in Scheme 3.

Compound ***5***. Compound **5** was purchased from a commercial vendor.

Compound ***6***. Compound **6** was synthesized as outlined in Scheme 4. 1-Chloro-2-fluoro-4-methoxy-5-nitrobenzene (**19**) was synthesized from commercially available 4-chloro-3-fluorophenol utilizing a known procedure.[40] Displacement of fluoro-containing **19** by 1,2-isopropylidenglycerin and subsequent reduction of the corresponding nitro derivative **20** by iron in acetic acid furnished aniline **21**. Acylation of **21** with chloroacetic chloride at 0 °C followed by S_n2 displacement with 6-mercaptonicotinic acid at 100 °C in a single pot led to compound **22**. Finally, protecting group removal with HCl yielded the desired product **6**.

Compound ***25***. Compound **25** was synthesized by Suzuki coupling as shown in Scheme 5.

Compound ***7***. Compound **7** was synthesized as shown in Scheme 6. 3,3′-Dihydroxylipropyl ether (**23**) was prepared from commercially available 3,3′-oxidipropionitrile utilizing a known procedure.[41] S_NAr reaction of fluoro-containing **19** by **23** in THF in the presence of NaH furnished compound **24** in 64% yield. The Mitsunobu coupling of alcohol **24** and phenol **25** using DIAD and triphenylphosphine afforded ether **26**. Subsequent nitro group reduction by hydrogenation in the presence of Pd−C yielded aniline **27**. Similar to the synthesis of compound **6**, treatment of **27** with chloroacetic chloride at 0 °C followed by displacement with 6-mercaptonicotinic acid methyl ester

Scheme 1. Synthesis of Compound 2[a]

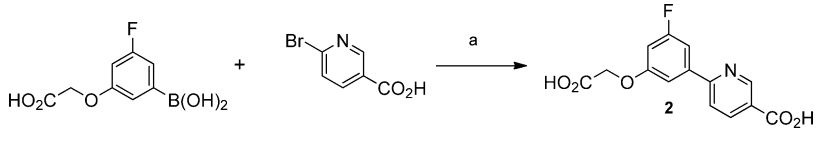

[a]Reagents and conditions: (a) $Pd(PPh_3)_4$, K_2CO_3, dioxane, microwave, 120 °C/20 min.

dx.doi.org/10.1021/jm3014844 | J. Med. Chem. XXXX, XXX, XXX−XXX

Scheme 2. Synthesis of Compound 3[a]

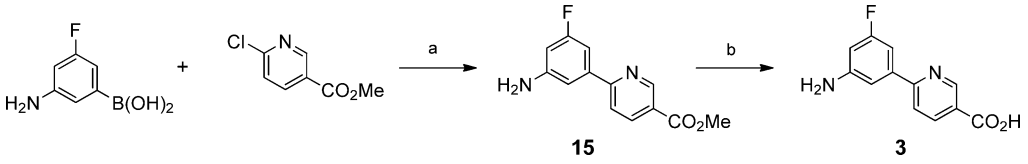

[a]Reagents and conditions: (a) $Pd(PPh_3)_4$, K_2CO_3, dioxane, 80 °C; (b) LiOH, $MeOH/H_2O$.

Scheme 3. Synthesis of Compound 4[a]

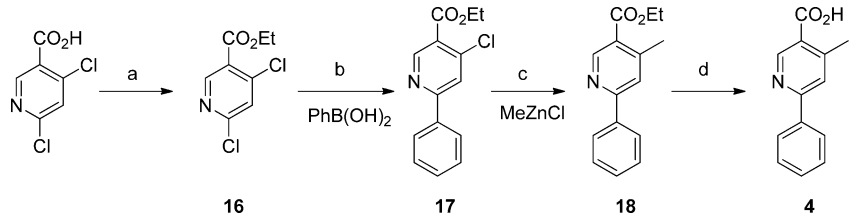

[a]Reagents and conditions: (a) $SOCl_2$ and then NaOEt; (b) $Pd(PPh_3)_4$, K_2CO_3, DME; (c) $Pd(PPh_3)_4$, THF; (d) LiOH, $EtOH/H_2O$.

Scheme 4. Synthesis of Compound 6[a]

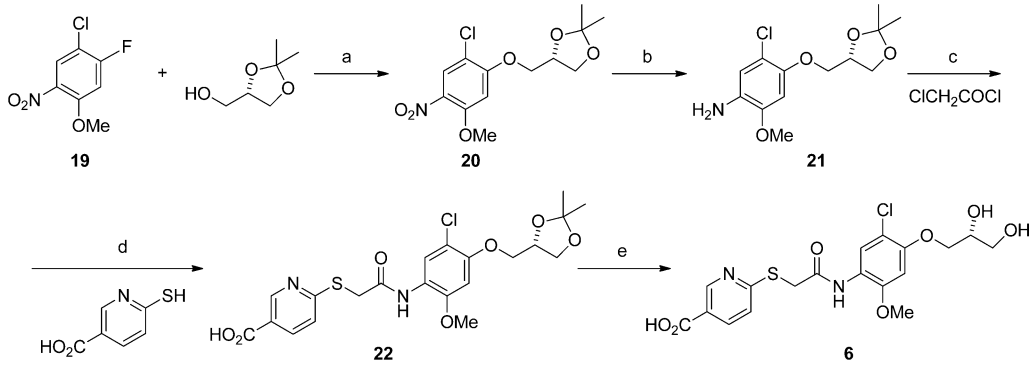

[a]Reagents and conditions: (a) K_2CO_3, DMF, 60 °C; (b) Fe, AcOH, reflux; (c) Et_3N, THF, 0 °C; (d) Et_3N, THF, 100 °C; (e) HCl, $MeOH/H_2O$, 50 °C.

Scheme 5. Synthesis of Compound 25

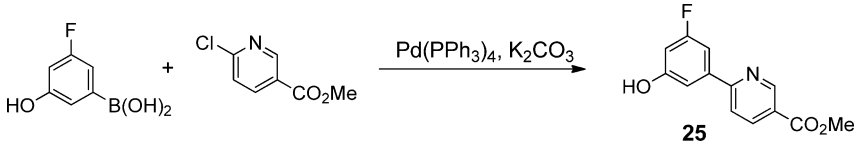

at 100 °C led directly to diester **28**. Subsequent hydrolysis with K_2CO_3 in $MeOH/H_2O$ at 80 °C furnished compound **7**.

Compound ***8***. 2,3:4,5-Bis-*O*-(1-methylethylidene)-D-mannitol (**29**) was prepared from 1,2:5,6-bis-*O*-(1-methylethylidene)-D-chiromannitol by $NaIO_4$ diol cleavage followed $NaBH_4$ reduction of the corresponding dialdehyde. With alcohol **29** in hand, compound **8** was synthesized in a similar manner to compound **7**, with the exception of an additional actonidie-deprotection after nitro reduction of compound **31** (Scheme 7).

Compound ***9***. PDC oxidation of intermediate alcohol **30** gave the corresponding aldehyde which was then converted to semiacetal **34** during workup and column purification in the presence of methanol. Reductive amination of **34** with aniline **15** in the presence of molecular sieves worked well to afford compound **35** in 70% yield. Finally, compound **9** was synthesized by following the same procedure as described in the synthesis of compound **8** (Scheme 8).

Compound ***40***. Synthesis of compound **40** is outlined in Scheme 9. 1-Chloro-2-fluoro-4-methoxy-5-nitrobenzene (**19**) was treated with KOH in $DMSO/H_2O$ at 100 °C to give phenol **37** in good yield. Nitro group reduction of **37** resulted in aniline **38**, which was used in the next step without further purification. In parallel, compound **39** was made by heating a mixture of ethyl 6-chloro-3-pyridinecarboxylate and mercaptoacetic acid neat at 100 °C. Subsequent DCC coupling of aniline **38** and acid **39** gave compound **40** in 46% yield.

Compound ***10***. As outlined in Scheme 10, acid **42** was prepared by reacting **25** with *tert*-butyl bromoacetate followed by a deprotection of the *tert*-butyl group. Coupling of acid **42** with 3-amino-1-propanol using EDCI and HOBT produced compound **43**. Mitsunobu coupling of **43** with phenol **40** gave diester **44**. Diester **44** was hydrolyzed with K_2CO_3 in $MeOH/H_2O$ to give the desired product **10**.

Compound ***11***. Starting from 1,2:5,6-bis-*O*-(1-methylethylidene)-D-chiroinositol, compound **11** was synthesized by the same procedure as described for compound **8** (Scheme 11).

Compound ***12***. Treatment of compound **36** with chloroacetyl chloride at 0 °C followed by mercaptopyridine at 100 °C led to

dx.doi.org/10.1021/jm3014844 | J. Med. Chem. XXXX, XXX, XXX−XXX

Scheme 6. Synthesis of Compound 7[a]

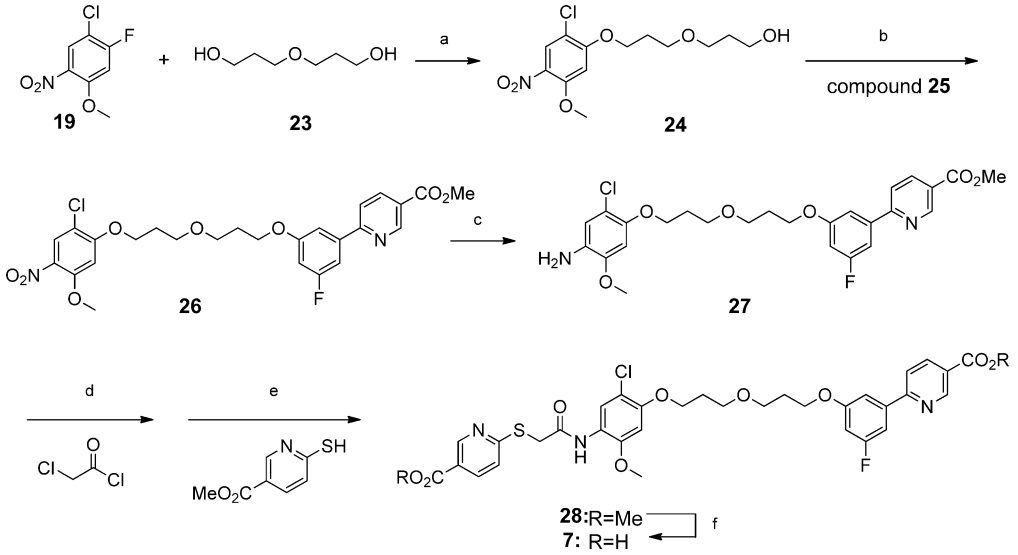

[a]Reagents and conditions: (a) NaH, THF, 60 °C; (b) DIAD, TPP, DCM, 0−60 °C; (c) H_2, Pd−C, MeOH, rt; (d) Et_3N, THF, 0 °C; (e) Et_3N, THF, 100 °C; (f) K_2CO_3, MeOH/H_2O, 80 °C.

Scheme 7. Synthesis of Compound 8[a]

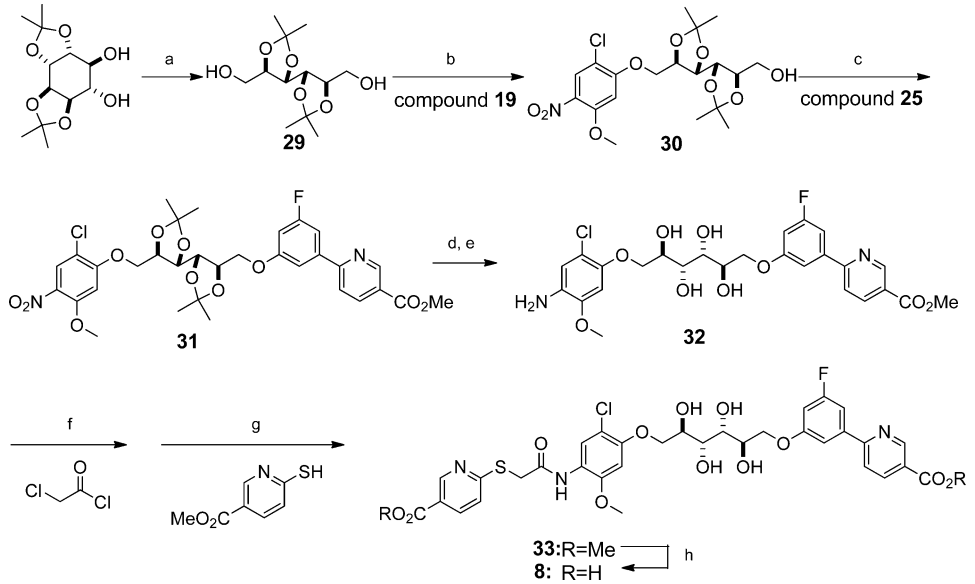

[a]Reagents and conditions: (a) (1) $NaIO_4$, acetone/H_2O; (2) $NaBH_4$; (b) NaH, THF, 60 °C; (c) DIAD, TPP, DCM, 0−60 °C; (d) Zn, NH_4Cl, acetone/water, rt; (e) HCl, MeOH; (f) Et_3N, THF, 0 °C; (g) Et_3N, THF, 100 °C; (h) K_2CO_3, MeOH/H_2O, 80 °C.

ester **50**. Hydrolysis of **50** with K_2CO_3 in MeOH/H_2O at 80 °C gave compound **12** as shown in Scheme 12.

Compound 13. As outlined in Scheme 13, compound **52** was synthesized via Suzuki coupling of 3-(Cbz-amino)-5-fluorophenylboronic acid and 2-bromopyridne followed by deprotection of the Cbz group under hydrogenation conditions. With aniline **52** in hand, compound **13** was synthesized by the same procedure as described for the synthesis of compound **9**.

Compound 56. Compound **56** was synthesized using the conditions reported in literature.[20]

Compounds 57 and 58. Compounds **57** and **58** were synthesized using published literature protocol.[42]

Biology. After determining that the compounds described here can directly inhibit LDH-A enzymatic activity, we next assessed whether they could reduce lactate levels in cancer cells. We assessed extracellular lactate levels in a Burkitt's lymphoma cell line (Ramos) treated with compounds **9**, **12**, **13**, an inactive compound **14**, or oxamate as a positive control (Figure 9). Compound **14** produced virtually no inhibition of lactate secretion, while oxamate reduced lactate levels to 48% and 56% of vehicle by 1 and 4 h, respectively. Like oxamate, compound **9** produced an initial inhibition to 56% by 1 h and to 68% by the later time point, reflecting a sustained effect. Compounds **12** and **13** more dramatically blocked lactate levels to 21% and 17%, respectively; however, both had begun to recover by 4 h to 61% and 35%. While the extent of cellular lactate inhibition does not directly correlate with LDH-A IC_{50}, we cannot rule out factors such as cell permeability, import and

dx.doi.org/10.1021/jm3014844 | J. Med. Chem. XXXX, XXX, XXX−XXX

Scheme 8. Synthesis of Compound 9[a]

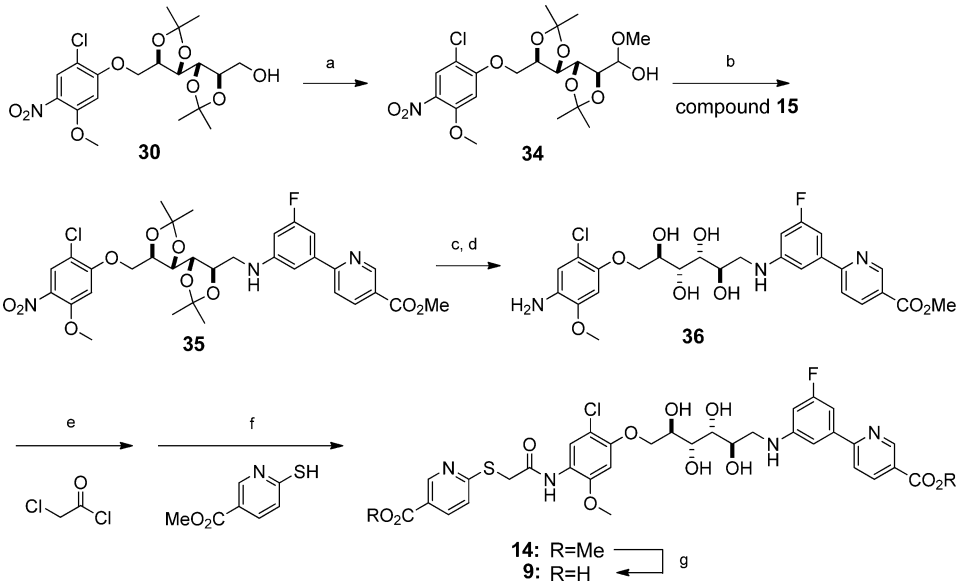

[a]Reagents and conditions: (a) PDC, MS, DCM, rt; (b) MS, DCM, $NaHB(OAc)_3$, rt; (c) Zn, NH_4Cl, acetone/water, rt; (d) HCl, MeOH; (e) Et_3N, THF, 0 °C; (f) Et_3N, THF, 100 °C; (g) K_2CO_3, MeOH/H_2O.

Scheme 9. Synthesis of Compound 40

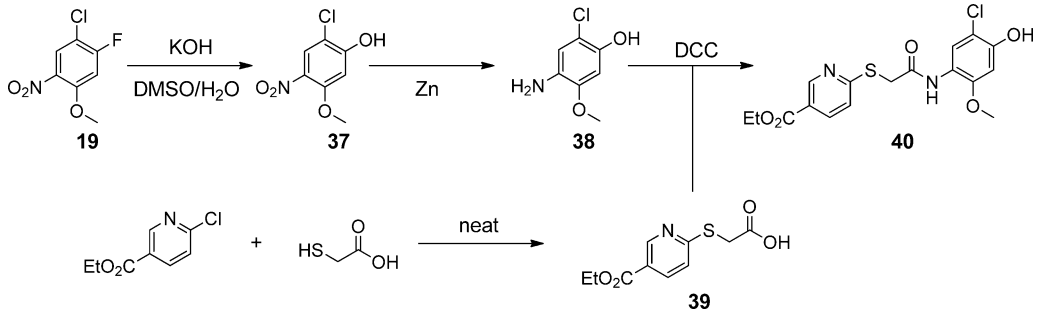

Scheme 10. Synthesis of Compound 10[a]

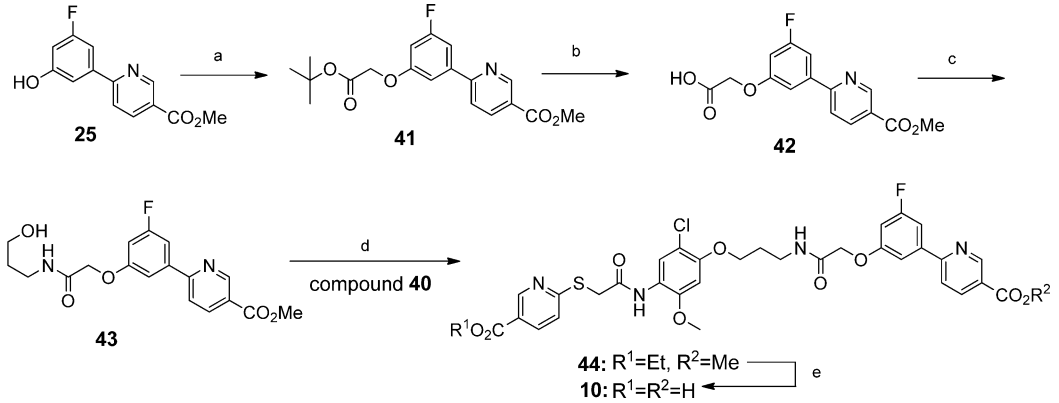

[a]Reagents and conditions: (a) *tert*-butyl 2-bromoacetate, K_2CO_3, THF, rt; (b) TFA, rt; (c) 3-amino-1-propanol, EDCI, HOBt, TEA, DMF, rt; (d) DIAD, TPP, THF 0 °C to rt; (e) K_2CO_3, 90 °C.

export processes, and degradation kinetics in shaping the cellular effects of these compounds. Taken together, all compounds except **14**, which lacks LDH-A activity, reduced cellular lactate levels reflecting activity against the LDH-A enzyme.

Evaluation of Enzyme Activity for Previously Published Inhibitors of LDH-A. During the course of the project we evaluated several previously published LDH-A inhibitors using enzymatic assays and biophysical methods. For the majority of compounds we were unable to reproduce key literature results under our experimental conditions. As an example, Supporting Information Figure 2SA shows the enzyme inhibition of compound **56** (FX11). While no enzyme inhibition

dx.doi.org/10.1021/jm3014844 | J. Med. Chem. XXXX, XXX, XXX−XXX

Scheme 11. Synthesis of Compound 11[a]

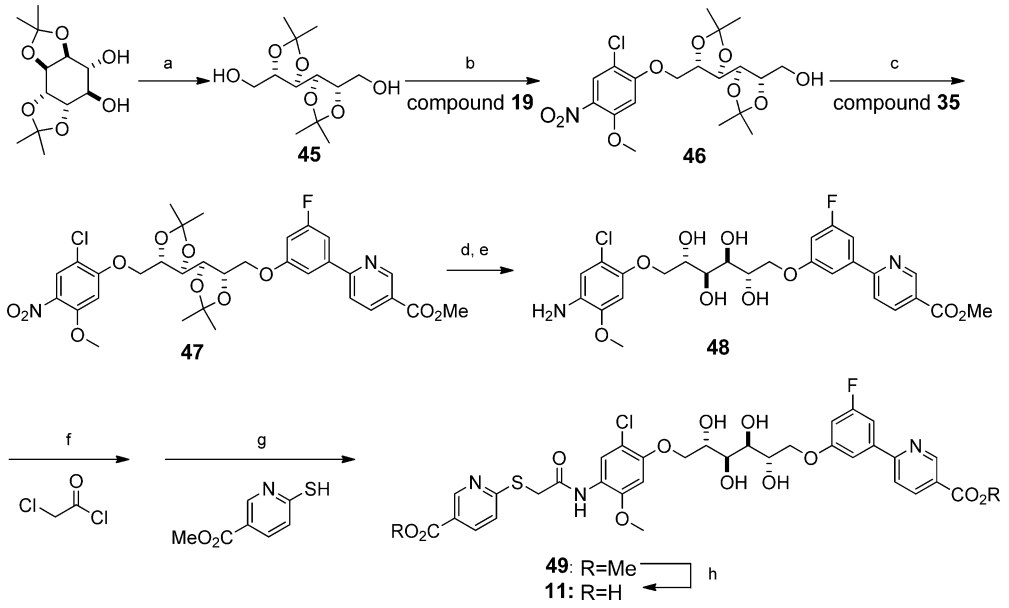

[a]Reagents and conditions: (a) (1) $NaIO_4$, acetone/H_2O; (2) $NaBH_4$; (b) NaH, THF, 60 °C; (c) DIAD, TPP, DCM, 0 to 60 °C; (d) Zn, NH_4Cl, acetone/water, rt; (e) HCl, MeOH; (f) Et_3N, THF, 0 °C; (g) Et_3N, THF, 100 °C; (h) K_2CO_3, MeOH/H_2O, 80 °C.

Scheme 12. Synthesis of Compound 12[a]

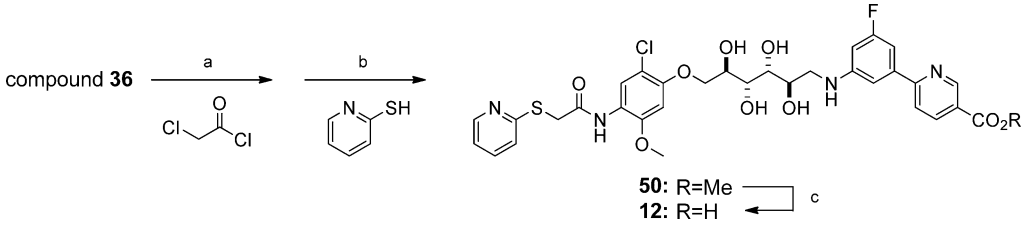

[a]Reagents and conditions: (a) Et_3N, THF, 0 °C; (f) Et_3N, THF, 100 °C; (g) K_2CO_3, MeOH/H_2O.

Scheme 13. Synthesis of Compound 13[a]

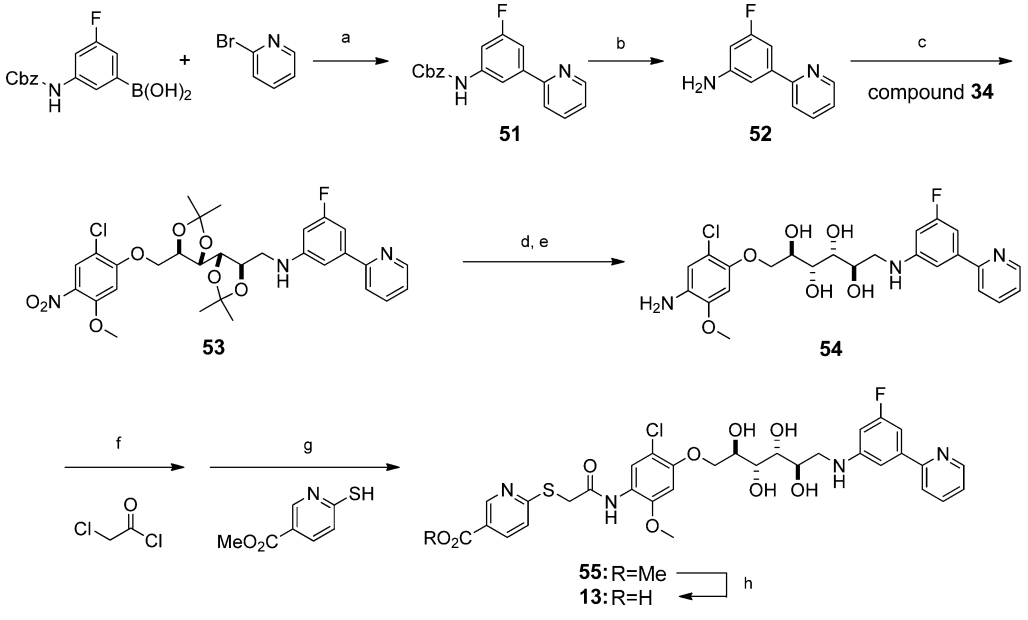

[a]Reagents and conditions: (a) $Pd(PPh_3)_4$, K_2CO_3, dioxane/H_2O; (b) H_2, Pd−C; (c) molecular sieves, DCM, $NaHB(OAc)_3$, rt; (d) Zn, NH_4Cl, acetone/water, rt; (e) HCl, MeOH; (f) Et_3N, THF, 0 °C; (g) B, Et_3N, THF, 100 °C; (h) K_2CO_3, MeOH/H_2O.

dx.doi.org/10.1021/jm3014844 | J. Med. Chem. XXXX, XXX, XXX−XXX

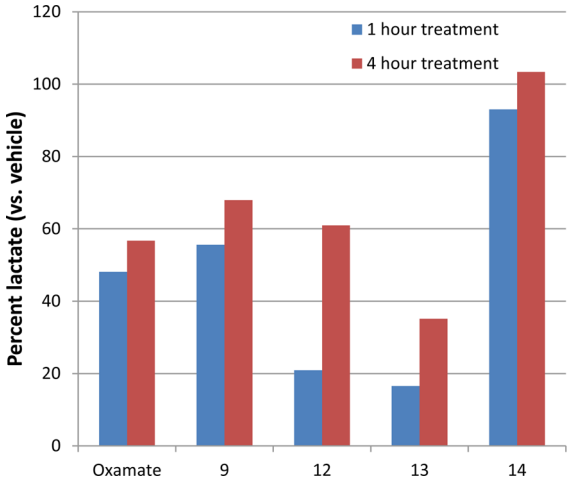

Figure 9. Inhibition of cellular lactate levels by compounds **9**, **12**, **13**, and **14**. Relative lactate levels were determined at 1 and 4 h treatments with the four compounds (200 μM) or the positive control oxamate (10 mM). A representative experiment is shown.

is observed in the presence of 0.1% Triton, the compound shows strong enzyme inhibition in the absence of detergent, with measured IC_{50} depending on experimental parameters, such as protein−compound incubation time, and ranging from ∼40 μM to >200 μM. These observations, together with the Hill coefficient, are indicative of enzyme inhibition by aggregation.[43]

This conclusion was further corroborated by SPR studies (Supporting Information Figure 2SB) which indicate superstoichiometic binding and slow on and off kinetics for this compound, implying unspecific binding due to compound aggregation.[44] Other previously reported compounds, such as compounds **57** and **58**, known as common ligand mimics (CLM)[42] showed similar behavior, as illustrated in Supporting Information Figure 3S. In the presence of detergent in the buffer, no enzyme inhibition was observed for those compounds when tested at up to 1 mM. Not surprisingly, attempts to produce cocrystal structures with those compounds were unsuccessful.

CONCLUSION

LDH-A, an enzyme is the glycolysis pathway, is considered a significant small-molecule oncology target in cancer metabolism. We demonstrate here the successful application of a fragment-based drug discovery strategy to find novel inhibitors of LDH-A. LDH-A proved to be a difficult target. It has a small substrate binding site formed in part by cofactor binding, leading to a need for inhibitors capable displacing the cofactor, and furthermore contains a polar and largely solvent-exposed binding site. Despite these challenges, a series of potent compounds was identified through growing and linking fragments. Binding of these potent linked fragment-based ligands extended through both cofactor and substrate binding sites, utilizing hydroxylated linkers to bind in the NADH pyrophosphate binding site. We demonstrated experimentally a lack of aggregator artifacts on binding of these compounds to LDH-A and confirmed their enzymatic activity with SPR binding assays where the ligands showed stoichiometric binding to the target. Additionally, we obtained several crystal structures of linked compounds bound to LDH-A. Finally, we demonstrated the ability of representative compounds to inhibit lactate levels in cells.

Our work highlights the power of fragment-based approaches in locating binding hot spots even in challenging targets and of the potency-enhancing effect of linking fragments. Although fragment growing itself failed to gain sufficient potency, ultimately a linking strategy proved to be successful as a means to enhance potency, resulting in potent and nonaggregating inhibitors of LDH-A. While we obtained compounds that demonstrated high potency in enzymatic assays, the physicochemical properties of the compounds are not optimal for cellular permeability. Further work remains to be done in making potent compounds with desirable ADME properties for this valuable target.

EXPERIMENTAL SECTION

NMR Spectroscopy. NMR experiments were performed at a temperature of 300 K on a Bruker Avance DRX 600 MHz spectrometer, equipped with a z-gradient 1.0 mm TXI microprobe and a Bruker SampleJet autosampler. STD-NMR experiments were recorded with 2 s saturation time, applying 50 ms Gaussian shaped pulses with a nominal flip angle of 720°. The frequency of the on-resonance irradiation was set to 0.8 ppm, and the off-resonance pulse was at 30 ppm. The residual water signal was suppressed using excitation sculpting. For the primary screen, rabbit LDH-A (Aldrich) was dissolved at 20 μM in D_2O based buffer containing 50 mM sodium phosphate, 100 mM NaCl, pH 7.4, and 0.33 mM of TSP as chemical shift reference. After addition of fragment from concentrated DMSO-d_6 stock solution at a final concentration of 2−3 mM per sample, about 10 μL of solution was transferred to 1.0 mm NMR tubes using a Gilson liquid handler. Samples contained up to 7% DMSO and were kept at room temperature until measured. Data sets shown were the average of 320 scans. All data processing was performed using the Bruker Topspin 1.3 software.

SPR. SPR studies were performed at room temperature on a BIAcore T100 or a Pioneer SensiQ instrument (as indicated). Human LDH-A was immobilized onto a CM5 chip via standard amine coupling which yielded ∼13000 RU of immobilized protein. Carbonic anhydrase II (Sigma) was used as reference protein. Binding of NADH to LDH-A was tested using 250 μM as the highest concentration in a 2-fold dilution series with nine concentrations in total. The running buffer contained 10 mM HEPES, 150 mM NaCl, and 3% DMSO. Each concentration was tested three times. An overlay of all the binding responses is shown in the Supporting Information (Figure 1S). The responses were well reproducible indicating that the LDH-A surface was active. The fit of the equilibrium response data to a 1:1 interaction model yielded a binding affinity of NADH of 13 μM at room temperature.

Crystallography. LDH from several organisms including human, rabbit, and dogfish were screened for a soaking suitable crystal system. Although we crystallized all the LDH proteins, only rabbit LDH gave well-diffracting crystals when cocrystallized with AMP.

Rabbit LDH, purchased from Sigma-Aldrich (catalog no. L2500), was purified from rabbit muscle containing predominantly LDH-5.The sequence of rabbit LDH-5 form is identical to its human counterpart (an all LDH-A tetramer) in the active site loop and near identical in the entire active site.[34] The purchased protein sample was then polished in a size-exclusion column in a buffer containing 50 mM Hepes, pH 7.5, 50 mM NaCl and 1 mM DTT. Cocrystals of rabbit LDH (25 mg/mL) with AMP (10 mM) were obtained at 4 °C in a condition containing 0.1 M Tris, pH 8.0, and 28% PEG 550 MME.

Soaking of the fragment hits and lead compounds was performed following a back-soaking procedure in which the LDH/AMP cocrystals were transferred to a fresh mother liquor for 2−15 h. Such a procedure is designed to allow the prebound AMP to dissociate from the enzyme. Then the apo crystals were soaked with inhibitors at 1−20 mM for up to 3 days and cryo-protected by 38% PEG 550 MME before flash-freezing with liquid nitrogen. Diffraction data were collected at 100 K on a Rigaku rotating anode and R-AXIS IV++ imaging system. The data were indexed and scaled using the HKL2000 package. The rabbit LDH crystals belong to $P21$ space group with cell dimensions of a = 83.9 Å, b = 139.7 Å, c = 138.9 Å, and β = 94.5°.

The structures were determined by molecular replacement with AMoRe using a tetramer from the structure of human LDH-A bound

dx.doi.org/10.1021/jm3014844 | J. Med. Chem. XXXX, XXX, XXX−XXX

with NADH and oxamate (PDB code 1i10) as a search model. There are two LDH-5 tetramers in the asymmetric unit. The structures were refined with CNX combined with model building in Quanta (Accelrys Inc.). The inhibitor molecules were built into the density after several cycles of refinement and model building. As a control, the structure of rabbit LDH determined after back-soaking showed AMP soaked out readily thus permitting subsequent inhibitor binding.

Molecular Modeling. The X-ray crystal structure of rabbit LDH-A with soaked-in AMP and the published ternary complex structure (PDB code 1i10) were used in modeling studies. To explore the binding cavity, SiteMap[35] and WaterMap were applied to the crystal structure. SiteMap was applied with default settings; cofactor and substrate were used to define binding site regions. WaterMap[45] was performed with default options on the crystal structure. An initial minimization and a molecular dynamics simulation was run for 9 ns on a solvated protein system in the absence of the ligand. The preparation of the protein for docking was performed with PrepWizard using the standard protocol, including the addition of hydrogens and the assignment of bond order and of correct protonation states. The hydrogen bonding network of the protein was optimized. Docking experiments were performed using Glide XP.[46] For substrate-site binders, a hydrogen-bond constraint to the Arg168 was used. For design of the linked molecules, the initial crystallographic poses of the two fragments were used as templates. Then a linker was built in and the resulting molecule minimized to obtain the optimal positioning of the linker. The fragments and ligands were treated with LigPrep[47] to obtain 3D structures, and protonation states were assigned using Epik. MM-GB/SA in Prime[48] was performed on top scoring ligand poses, with default settings.

Biology. The human Burkitt's lymphoma cell line Ramos (American Type Cell Culture, Manassus, VA, catalog no. CRL-1596) was plated at 5×10^6 cells/mL and treated with 200 μM **9**, **12**, **13**, and **14**, 10 mM oxamate, or vehicle. Then 5 μL of supernatant was harvested, and lactate levels were determined after 1 and 4 h of treatment using a two-step lactate assay (Trinity Biotech, Wicklow, Ireland, catalog no. 735-10) (Supporting Information Figure 4S). Both time points were determined to be within the linear range of the reaction. A control reaction using purified lactate instead of supernatant was performed to confirm that the compounds do not affect lactate oxidase or peroxidase activity.

Chemistry. General Remarks. Commercially available chemicals and solvents were purchased and used without further purification. ^{1}H NMR spectra were recorded on a Bruker Avance 400 spectrometer. Chemical shifts (δ) are reported relative to $CDCl_3$ at 7.26 ppm or DMSO-d_6 at 2.50 ppm as an internal standard. Mass spectra were recorded on a Waters Micromass ZQ spectrometer. HPLC was performed on an Agilent 1100 HPLC system. All tested compounds were purified to >95% purity as determined by ^{1}H NMR and by HPLC (C-18 column, MeCN/H_2O with 0.1% TFA as the mobile phase).

Compound 2. To a microwaveable test tube was loaded a mixture of 6-bromonicotinic acid (101 mg, 0.5 mmol), 3-(carboxymethoxy)-5-fluorophenylboronic acid (105 mg, 0.5 mmol), and $Pd(PPh_3)_4$ (60 mg, 0.05 mmol). This septum-capped tube was degassed via three cycles of vacuum-refilling of N_2. To this tube was added dioxane (3 mL, Aldrich Sureseal bottle) and 2 M aqueous K_2CO_3 (2 mL, predegassed). The resulting suspension was heated under microwave at 120 °C for 20 min. The reaction was quenched with addition of 2 N aqueous HCl, and the solvents were removed on rotavap. The crude solid was dissolved in DMSO, and the filtered solution was subjected to preparative HPLC purification to furnish **2** as white solid (20 mg, 14%). ^{1}H NMR (DMSO-d_6, 400 MHz) δ 9.14 (dd, 1H, J = 2.0, 0.8 Hz), 8.33 (dd, 1H, J = 8.0, 2.0 Hz), 8.16 (d, 1H, J = 8.8 Hz), 7.60 (s, 1H), 7.57 (d, 1H, J = 2.4 Hz), 6.96 (d, 1H, J = 10.8 Hz), 4.80 (s, 2H). MS (ES+) m/z 292 (M + 1).

Compound 15. A mixture of methyl 6-chloronicotinate (1.0 g, 5.83 mmol), 3-amino-5-fluorophenylboronic acid (0.9 g, 1.0 mmol), $Pd(PPh_3)_4$ (360 mg), dioxane (10 mL), and water (5 mL) was degassed and then heated at 100 °C for 15 min. The reaction mixture was diluted with ethyl acetate (10 mL). Organic layer was separated and evaporated. The residue was purified by column chromatography (elution, heptane/ethyl acetate = 1:1) to give the title compound **15** (1.1 g, 77%) as an off white solid.

^{1}H NMR (400 MHz, $CDCl_3$) δ 9.18 (dd, J = 2.0, 0.8 Hz, 1H), 9.26 (dd, J = 8.4, 2.0 Hz, 1H), 7.66 (dd, J = 8.4, 0.8 Hz, 1H), 7.19 (s, 1H), 7.13 (t, J = 1.6 Hz, 1H), 7.01 (ddd, J = 10.0, 2.0, 1.6 Hz, 1H), 6.41 (ddd, J = 10.0, 2.4, 2.0 Hz, 1H), 3.90 (s, 3H).

Compound 3. A suspension of compound **15** (40 mg, 0.16 mmol) in MeOH (1.0 mL) was treated with LiOH (2 equiv) and drops of water at room temperature for 1 h. Formic acid (drops) was added, and then solvent was evaporated. The residue was purified by preparative HPLC to give the title compound (25 mg, 66%) as a light yellow solid.

Compound 16. The 4,6-dichloronicotinic acid (9.5 g, 49.5 mmol) was refluxed in 100 mL of thionyl chloride for 2 h and evaporated. The residue was dissolved in 100 mL of anhydrous ethanol, and sodium ethoxide (3.70 g, 54 mmol) was added. The reaction was stirred at room temperature overnight and filtered. The filtrate was evaporated and chromatographed (heptane/ethyl acetate 10:1) to give an oil, 8.8 g, in 81% yield. ^{1}H NMR (ppm) ($CDCl_3$) 8.77 (s, 1H), 7.39 (s, 1H), 4.36 (q, J = 7.2 Hz, 2H), 1.34 (t, J = 7.2 Hz, 3H).

Compound 17. Compound **16** (3.3 g, 15.0 mmol) and $Pd(PPh_3)_4$ (303.6 mg) were stirred in 13 mL of dimethoxyethane at room temperature for 15 min. To this suspension was then added phenylboronic acid (1.74 g, 14.2 mmol) in 15 mL of isopropanol and 13.2 mL of 2.0 M K_2CO_3. The mixture was stirred at 95 °C for 1 h. After evaporation, the mixture was worked up with saturated $NaHCO_3$ and DCM and chromatographed (EtOAc/heptane = 1:10) to give a white solid, 2.4 g, in 61% yield. ^{1}H NMR (ppm) ($CDCl_3$) 9.04 (s, 1H), 7.94 (m, 2H), 7.74 (s, 1H), 7.44 (m, 3H), 4.38 (q, J = 7.2 Hz, 2H), 1.34 (t, J = 7.2 Hz, 3H) .

Compound 18. Compound **17** (127 mg, 0.485 mmol) was dissolved in 10 mL of THF, and $Pd(PPh_3)_4$ (30 mg, 0.025 mmol) was added. The mixture was stirred under N_2 for 5 min to get a clear solution. Methylzinc chloride (2.0 M in THF, 0.5 mL, 1.0 mmol) was added at room temperature, and the mixture was stirred at 70 °C overnight. Another 1.0 mL of CH_3ZnCl and $Pd(PPh_3)_4$ (40 mg) were added, and the stirring was continued at 80 °C overnight. The mixture was evaporated and worked up with saturated NH_4Cl and DCM and purified with flash chromatography (EtOAc/heptane = 1:10) to give an oil, 106 mg, in 91% yield. ^{1}H NMR (ppm) ($CDCl_3$) 9.10 (s, 1H), 7.95 (m, 2H), 7.52 (s, 1H), 7.42 (m, 3H), 4.34 (q, J = 7.2 Hz, 2H), 2.62 (s, 3H), 1.34 (t, J = 7.2 Hz, 3H).

Compound 4. Compound **18** (103 mg, 0.43 mmol) was dissolved in 10 mL of 2.0 M Na_2CO_3 and 10 mL of EtOH. The mixture was stirred at room temperature for 15 min, and LiOH (30 mg) was added. The mixture was stirred at room temperature for 30 min and evaporated to half of the volume. Then 10 mL of water was added, and the solution was washed with ether (10 mL) and DCM (5 mL). The solution was adjusted to pH 5 with concentrated HCl to get a precipitate. The precipitate was filtered and the solid was washed with water and ether and dried to give a white solid, 57.9 mg, in 62% yield. ^{1}H NMR (ppm) (DMSO) 13.20 (s, 1H), 9.02 (s, 1H), 8.15 (m, 2H), 7.96 (s, 1H), 7.47–7.55 (m, 3H), 2.64 (s, 3H).

Compound 19. Compound **19** was made from 3-fluoro-4-chlorophenol as reported.[40]

Compound 20. A mixture of compound **19** (205 mg, 1.0 mmol) and 1,2-isopropylidenglycerin (145 mg, 1.1 mmol) in DMF (1.0 mL) was treated with potassium carbonate (1.0 g) at 60 °C for 10 min. The mixture was diluted with DCM (3.0 mL), and then the solid was filtered off. The solution was evaporated, and the residue was used for the next step.

Compound 21. The residue **20** was dissolved in acetic acid (2.0 mL) and then treated with iron (0.5 g, powder). The mixture was heated to reflux and then diluted with ethyl acetate (4.0 mL). After filtration, solvent was evaporated and the residue was purified with a preparative TLC plate (elution, DCM/MeOH = 100:3) to give the title compound product **21** (120 mg, 42% two steps) as an off white solid.

Compound 6. To a solution of **21** (57 mg, 0.20 mmol) in THF (1.0 mL) and triethylamine (0.01 mL) was added chloroacetyl chloride (2.0 M solution in THF) at 0 °C, monitoring the reaction with HPLC until the starting material disappeared. 6-Mercaptonicotinic acid (120 mg, 0.77 mmol) was introduced. The resulting mixture was heated in a sealed tube at 100 °C for 5 min. Solvent was evaporated, and the residue was treated with HCl in dioxane (1.0 mL) at room temperature

dx.doi.org/10.1021/jm3014844 | J. Med. Chem. XXXX, XXX, XXX–XXX

for 6 h. Solvent was evaporated and the residue was purified with preparative HPLC chromatography to give the title compound **6** (31 mg, 35%) as an off white solid. MS (ES^+) m/z (M + 1) 443; ^{1}H NMR (400 MHz, DMSO) δ 9.67 (s, 1H), 8.95 (d, J = 1.6 Hz, 1H), 8.17 (s, 1H), 8.12 (dd, J = 8.4, 2.4 Hz, 1H), 8.05 (s, 1H), 7.54 (d, J = 8.4 Hz, 1H), 6.86 (s, 1H), 4.13 (s, 2H), 4.07 (dd, J = 10.0, 4.4 Hz, 1H), 4.00 (dd, J = 10.0, 6.4 Hz, 1H), 3.85 (s, 3H), 3.81(quint, J = 5.6 Hz, 1H), 3.49 (dd, J = 10.8, 5.6 Hz, 1H), 4.07 (dd, J = 10.8, 5.6 Hz, 1H).

Compound 23. Compound **23** was synthesized according to the procedure described.[41]

Compound 24. A solution of 3,3′-dihydroxydipropyl ether **15** (500 mg, 3.73 mmol) in THF (10 mL) was treated with NaH (77 mg, 1.9 mmol, 60% in mineral oil) at room temperature and stirring for 1 h. 2-Nitro-4-chloro-5-fluoroanisole (400 mg, 1.62 mmol) was added, and the resulting mixture was warmed to 60 °C for 15 min. Solvent was evaporated and the residue was purified by a flash column chromatography (elution, DCM/MeOH = 100:0 to 5) to give the title compound (330 mg, 64%) as a yellow solid. ^{1}H NMR (400 MHz, $CDCl_3$) δ 8.09 (s, 1H), 6.57 (s, 1H), 4.22 (t, J = 6.0 Hz, 2H), 4.00 (s, 3H), 3.77 (t, J = 6.0 Hz, 2H), 3.69 (t, J = 6.0 Hz, 2H), 3.66 (t, J = 6.0 Hz, 2H), 2.16 (quint, J = 6.0 Hz, 2H), 1.85 (quint, J = 6.0 Hz, 2H).

Compound 25. 2-Chloro 6-methylpyridinylcarboxylate (344 mg, 2.0 mmol), 3-fluoro-5-hydroxyphenylboronic acid (406 mg, 2.6 mmol), and $Pd(PPh_3)_4$ (110 mg, 0.095 mmol) were weighed into a 10 mL round-bottom flask under Ar. Dioxane (12 mL) was added to the mixture, followed by 2.5 mL of K_2CO_3 solution (1.6 M, 4 mmol). The content was stirred at 80 °C overnight. To the mixture were added EtOAc and 5% citric acid. The organic layer was separated, and the aqueous layer was extracted with more EtOAc. Combined organic layers were dried over Na_2SO_4, concentrated. Crude product was purified by flash chromatography (EtOAc/hexanes) to give 350 mg product as a white solid (yield, 54%).

Compound 26. To a solution of triphenylphosphine (613 mg, 2.34 mmol) in THF (3.0 mL) was added DIAD (400 uL, 2.0 mmol) at −20 °C, and the mixture was warmed to 0 °C for 10 min. A mixture of compound **16** (500 mg, 1.56 mmol) and compound **35** (386 mg, 1.56 mmol) was introduced. After 10 min at room temperature, the reaction vial was capped and heated at 60 °C for 10 min. Solvent was evaporated and the residue was purified by flash column chromatography (elution, DCM/MeOH = 100:3) to give the title compound (560 mg, 65%) as a white solid. ^{1}H NMR (400 MHz, $CDCl_3$) δ 9.30 (dd, J = 2.0, 0.8 Hz, 1H), 8.40 (dd, J = 8.0, 2.0 Hz, 1H), 8.07 (s, 1H), 7.80 (dd, J = 8.4, 0.8 Hz, 1H), 7.49 (t, J = 1.6 Hz, 1H), 7.35 (ddd, J = 9.6, 2.0, 1.2 Hz, 1H), 6.72 (dt, J = 10.4, 2.4 Hz, 1H), 6.54 (s, 1H), 4.24 (t, J = 6.0 Hz, 2H), 4.18 (t, J = 6.0 Hz, 2H), 4.04 (s, 3H), 3.95 (s, 3H), 3.74 (t, J = 6.0 Hz, 2H), 2.20 (quint, J = 6.0 Hz, 2H), 2.13 (quint, J = 6.0 Hz, 2H).

Compound 27. A solution of **26** (279 mg, 0.51 mmol) in methanol (8 mL) was charged with Pd−C (0.5 g). The mixture was hydrogenated under a hydrogen balloon for 15 min. The catalyst was filtered off and solvent was evaporated to give the title compound (230 mg, 87%) as a yellow solid. ^{1}H NMR (400 MHz, $CDCl_3$) δ 9.25 (dd, J = 2.0, 0.8 Hz, 1H), 8.33 (dd, J = 8.4, 2.4 Hz, 1H), 7.74 (dd, J = 8.4, 0.8 Hz, 1H), 7.41 (t, J = 1.6 Hz, 1H), 7.33 (ddd, J = 9.6, 2.0, 1.6 Hz, 1H), 6.69 (dt, J = 10.0, 2.4 Hz, 1H), 6.68 (s, 1H), 6.48 (s, 1H), 4.10 (t, J = 6.0 Hz, 2H), 4.04 (t, J = 6.0 Hz, 2H), 3.97 (s, 3H), 3.78 (s, 3H), 3.67 (t, J = 6.0 Hz, 2H), 3.65 (t, J = 6.4 Hz, 2H), 2.10−2.02 (m, 4H).

Compound 28. To a solution of **27** (230 mg, 0.44 mmol) in THF (4.0 mL) and triethylamine (0.3 mL) was added chloroacetyl chloride (2.0 M in THF) at −20 °C, monitoring the reaction with HPLC until the starting material disappeared. 6-Mercaptonicotinic acid methyl ester (105 mg, 0.62 mmol) was introduced. The resulting mixture was heated in a sealed tube at 100 °C for 5 min. Solvent was evaporated and the residue was purified by using two preparative TLC plates (elution, DCM/THF = 100:5) to give the title compound (180 mg, 56%) as a yellow solid. ^{1}H NMR (400 MHz, $CDCl_3$) δ 9.57 (s, 1H), 9.27 (dd, J = 2.4, 0.8 Hz, 1H), 9.11 (dd, J = 2.4, 0.8 Hz, 1H), 8.39 (s, 1H), 8.37 (dd, J = 8.4, 2.4 Hz, 1H), 8.13 (dd, J = 4.4, 2.0 Hz, 1H), 7.76 (dd, J = 8.4, 0.8 Hz, 1H), 7.42 (t, J = 1.2 Hz, 1H), 7.35 (dd, J = 8.4, 0.8 Hz, 1H), 7.33 (m, 1H), 6.68 (dt, J = 8.4, 2.0 Hz, 1H), 6.44 (s, 1H), 4.12 (t, J = 6.4 Hz, 2H), 4.07 (t, J = 6.0 Hz, 2H), 4.00 (s, 3H), 3.99 (s, 2H), 3.97 (s, 3H), 3.74 (s, 3H), 3.68 (t, J = 6.0 Hz, 2H), 3.66 (t, J = 6.4 Hz, 2H).

Compound 7. A solution of **28** (125 mg, 0.17 mmol) in methanol (0.5 mL) was treated with potassium carbonate (250 mg) and water (drops) in a capped vial at 80 °C for 5 min. The organic layer was transferred to a new vial and diluted with water (2.0 mL). The mixture was then treated with formic acid to pH 3−4. The precipitate was collected by filtration and washed with methanol (1.5 mL) to give the title compound **7** (58 mg, 49%) as a yellow solid. MS (ES^+) m/z (M + 1) 700; ^{1}H NMR (400 MHz, DMSO) δ 13.45 (br, 1H), 9.61 (s, 1H), 9.12 (dd, J = 2.4, 0.8 Hz, 1H), 8.93 (d, J = 1.2 Hz, 1H), 8.31 (dd, J = 8.4, 2.0 Hz, 1H), 8.12 (dd, J = 8.4, 0.8 Hz, 1H), 8.10 (dd, J = 8.4, 2.4 Hz, 1H), 8.05 (s, 1H), 7.55−7.49 (m, 3H), 6.91 (dt, J = 9.2, 2.4 Hz, 1H), 6.78 (s, 1H), 4.14−4.09 (m, 6H), 3.78 (s, 3H), 3.60−3.55 (m, 4H), 2.02−1.93 (m, 4H).

Compound 29. To a solution of 1,2:5,6-bis-*O*-(1-methylethylidene)-D-chiroinositol (2.0 g, 7.7 mmol) in acetone (10 mL) was added $CaCO_3$ (1.0 g), and the resulting mixture was treated with $NaIO_4$ (2.0 g) in water (20 mL) at room temperature for 2 h. The mixture was extracted with EtOAc (2 × 10 mL), and the combined organic solution was dried and evaporated for the next step. The residue was dissolved in MeOH (20 mL) and treated with NaBH4 (1.0 g, excess) at room temperature for 30 min. After aqueous workup, the product was purified by a flash column (DCM/MeOH = 100:8) to give a white solid (1.3 g, 65%).

Compound 30. A solution of 2,3:4,5-bis-*O*-(1-methylethylidene)-D-mannitol **29** (5.5 g, 26.8 mmol) in THF (100 mL) was treated with sodium hydride (0.8 g, 20 mmol, 60% in mineral oil) at room temperature and stirring for 1 h. 2-Nitro-4-chloro-5-fluoroanisole (4.0 g, 19.5 mmol) was added, and the resulting mixture was warmed to 60 °C for 15 min. Solvent was evaporated and the residue purified with a flash column chromatography (elution, DCM/MeOH = 100:0 to 5) to give the title compound (4.4 g, 50%) as a yellow solid. ^{1}H NMR(400 MHz, $CDCl_3$) δ 8.10 (s, 1H), 6.64 (s, J = 8.4, 1H), 6.70 (ddd, J = 10.8, 6.4, 4.8 Hz, 1H), 4.56 (dd, J = 6.4, 4.4 Hz, 1H), 4.45−4.39 (m, 2H), 4.33 (dd, J = 11.6, 5.2 Hz, 1H), 4.20 (dd, J = 9.2, 4.4 Hz), 4.01 (s, 3H), 3.84−3.76 (m, 2H), 2.39 (dd, J = 7.2, 5.6 Hz, 1H), 1.57 (s, 3H), 1.51 (s, 3H), 1.46 (s, 3H), 1.27 (s, 3H).

Compound 31. To a solution of triphenylphosphine (150 mg, 0.57 mmol) in DCM (3.9 mL) was added DIAD (100 uL, 0.51 mmol) at −20 °C, and the mixture was warmed to 0 °C for 10 min. A mixture of compounds **30** (168 mg, 0.37 mmol) and **25** (90 mg, 0.36 mmol) was introduced. After 10 min at room temperature, the reaction vial was capped and heated at 60 °C for 10 min. Solvent was evaporated and the residue was purified with two preparative TLC plates (elution, DCM/AcOEt = 100:10) to give the title compound (152 mg, 61%) as a white solid. ^{1}H NMR(400 MHz, $CDCl_3$) δ 9.29 (dd, J = 2.4, 0.8 Hz, 1H), 8.39 (dd, J = 8.4, 2.0 Hz, 1H), 8.08 (s, 1H), 7.78 (dd, J = 8.4, 0.8 Hz, 1H), 7.48 (dd, J = 2.0, 1.6 Hz, 1H), 7.39 (ddd, J = 9.6, 2.4, 1.6 Hz, 1H), 6.75 (ddd, J = 10.0, 2.4, 2.0 Hz, 1H), 6.63 (s, 1H), 4.65−4.70 (m, 2H), 4.63 (dd, J = 6.0, 4.4 Hz, 1H), 4.53 (dd, J = 6.0, 4.4 Hz, 1H), 4.45 (dd, J = 9.6, 7.6 Hz, 1H), 3.34 (dd, J = 10.0, 7.6 Hz, 1H), 4.20 (dt, J = 9.2, 4.4 Hz, 2H), 4.01 (s, 3H), 4.00 (s, 3H), 1.54 (s, 3H), 1.53 (s, 3H), 1.36 (s, 3H), 1.33 (s, 3H).

Compound 32. A suspension of compound **31** (550 mg, 0.81 mmol) in acetone (5.0 mL) and water (0.5 mL) was treated with zinc (1.0 g, excess) and ammonium chloride (0.5 g) at room temperature for 15 min. Organic layer was transferred to a new vial, and the residue was extracted with ethyl acetate (3.0 mL). Combined organic solution was dried and evaporated. The residue was purified using flash column chromatography (elution, DCM/MeOH = 100:3) to give the title compound (410 mg, 78%) as an off white solid. ^{1}H NMR(400 MHz, $CDCl_3$) δ 9.27 (dd, J = 2.4, 0.8 Hz, 1H), 8.36 (dd, J = 8.0, 2.0 Hz, 1H), 7.60 (dd, J = 8.4, 0.8 Hz, 1H), 7.45 (t, J = 1.6 Hz, 1H), 7.40 (ddd, J = 9.2, 2.0, 1.2 Hz, 1H), 6.74 (ddd, J = 10.0, 2.4, 2.0 Hz, 1H), 6.70 (s, 1H), 6.54 (s, 1H), 4.72 (dd, J = 11.6, 6.0 Hz, 1H), 4.63 (t, J = 6.4 Hz, 1H), 4.62−4.59 (m, 1H), 4.59 (dd, J = 6.4, 6.0 Hz, 1H), 4.29 (dd, J = 9.6, 6.4 Hz, 1H), 4.25 (dd, J = 9.6, 7.6 Hz, 1H), 4.15 (dd, J = 9.6, 5.2 Hz, 1H), 4.01 (dd, J = 9.6, 4.4 Hz, 1H), 3.99 (s, 3H), 3.83 (s, 3H), 1.55 (s, 3H), 1.54 (s, 3H), 1.40 (s, 3H), 1.39 (s, 3H).

dx.doi.org/10.1021/jm3014844 | J. Med. Chem. XXXX, XXX, XXX−XXX

Compound 33. A solution of **32** (220 mg, 0.39 mmol) in THF (3.0 mL) and triethylamine (60 μL) was treated with chloroacetyl chloride (250 uL, 2.0 M solution in THF). The mixture was warmed up to room temperature for 5 min, and then 6-mercaptonicotinic acid methyl ester (130 mg, 0.77 mmol) was added. The mixture was heated in a sealed tube at 100 °C for 5 min. Solvent was evaporated and the residue purified with a preparative TLC plate (DCM/MeOH = 100:8) to give an off white solid (140 mg, 46%). ^{1}H NMR (400 MHz, DMSO) δ 9.63 (s, 1H), 9.18 (dd, J = 2.0, 0.8 Hz, 1H), 8.96 (d, J = 1.2 Hz, 1H), 8.37 (dd, J = 8.4, 2.0 Hz, 1H), 8.21 (dd, J = 8.4, 0.8 Hz, 1H), 8.14 (dd, J = 8.4, 2.0 Hz, 1H), 8.04 (s, 1H), 7.63 (t, J = 2.0 Hz, 1H), 7.58 (d, J = 8.4 Hz, 1H), 7.57 (dm, J = 9.2 Hz, 1H), 6.98 (dt, J = 9.2, 2.4 Hz, 1H), 6.90 (s, 1H), 4.95 (d, J = 6.0 Hz, 1H), 4.9 (d, J = 6.0 Hz, 1H), 4.45 (d, J = 6.4 Hz, 1H), 4.43 (d, J = 6.0 Hz, 1H), 4.36−4.31 (m, 2H), 4.16 (s, 2H), 4.14 (dd, J = 9.2, 5.2 Hz, 1H), 4.14−4.11 (m, 2H), 3.93 (s, 3H), 3.88 (s, 3H), 3.86 (s, 3H), 3.87−3.77 (m, 2H).

Compound 8. A solution of **33** (80 mg, 0.10 mmol) in methanol (0.5 mL) was treated with potassium carbonate (300 mg) and water (0.2 mL) in a capped vial at 80 °C for 5 min. Organic layer was transferred to a new vial, and then drops of formic acid were added. The pH was checked to ensure that the mixture is mildly acidic. The mixture was purified using preparative HPLC to give the title compound (31.5 mg, 41%) as an off white solid. MS (ES$^+$) m/z (M + 1) 748; ^{1}H NMR (400 MHz, DMSO) δ 13.36 (br, 1H), 9.67 (s, 1H), 9.14 (dd, J = 2.0, 0.8 Hz, 1H), 8.94 (d, J = 1.6 Hz, 1H), 8.32 (dd, J = 8.4, 2.0 Hz, 1H), 8.15 (d, J = 8.0 Hz, 1H), 8.11 (dd, J = 8.4, 2.0 Hz, 1H), 8.05 (s, 1H), 7.61 (d, J = 1.6 Hz, 1H), 7.54 (dt, J = 9.6, 2.0 Hz, 1H), 6.95 (dt, J = 9.6, 2.4 Hz, 1H), 6.89 (s, 1H), 4.93−4.90 (m, 2H), 4.43 (m, 2H), 4.32 (t, J = 8.0 Hz, 2H), 4.14−4.10 (m, 2H), 4.13 (s, 2H), 3.88−3.77 (m, 2H), 3.85 (s, 3H).

Compound 34. To a solution of **30** (2.0 g, 4.5 mmol) in DCM (80 mL) was added molecular sieves (3.0 g, 4 Å) and PDC (3.0 g, 8.0 mmol). The mixture was stirred at room temperature for 2 h and then diluted with ether (100 mL). The mixture was filtered through a Celite pad, and solvent was evaporated. The residue was purified with silica gel column chromatography (elution, DCM/MeOH = 100:0 to 2) to give the title compound (1.4 g, 70%) as a light yellow solid. ^{1}H NMR (400 MHz, $CDCl_3$) δ 8.08 (s, 1H), 6.62 (s, 1H), 4.83 (dd, J = 6.8, 2.4 Hz, 1H), 4.72 (dd, J = 11.2, 4.4 Hz, 1H), 4.69−4.65 (m, 1H), 4.49 (dd, J = 6.8, 2.4 Hz, 1H), 4.41 (dd, J = 9.2, 7.6 Hz, 1H), 4.24−4.19 (m, 1H), 4.18 (s, 1H), 4.15 (s, 1H), 3.99 (s, 3H), 3.47 (s, 3H), 1.57 (s, 3H), 1.50 (s, 3H), 1.45 (s, 3H), 1.20 (s, 3H),

Compound 35. To a solution of **34** (450 mg, 1.0 mmol) in DCM (5.0 mL) were added molecular sieves (0.5 g) and compound **15** (250 mg, 1.0 mmol). The mixture was stirred for 5 min, and $NaBH(OAc)_3$ (0.5 g, 2.3 mmol) was added. The resulting mixture was stirred at room temperature for 2 h and diluted with aqueous sodium bicarbonate. Organic layer was dried, evaporated and the residue was purified with silica gel column chromatography (elution, DCM/MeOH = 100:3 to 5) to give the title compound **35** (470 mg, 70%) as a yellow solid. ^{1}H NMR (400 MHz, $CDCl_3$) δ 9.27 (dd, J = 2.4, 0.8 Hz, 1H), 8.35 (dd, J = 8.4, 2.0 Hz, 1H), 8.08 (s, 1H), 7.75 (dd, J = 7.6, 0.8 Hz, 1H), 7.29 (s, 1H), 7.20 (t, J = 2.0 Hz, 1H), 7.06 (dd, J = 9.6, 2.0 Hz, 1H), 6.63 (s, 1H), 6.44 (dt, J = 10.8), 6.68 (dt, J = 10.0, 4.4 Hz, 1H), 4.52−4.46 (m, 4H), 4.43 (dd, J = 9.2, 8.4 Hz, 1H), 4.26 (dt, J = 9.2, 1.6 Hz, 1H), 4.19 (dd, J = 9.6, 4.4 4.00 (s, 6H), 3.56−3.52 (m, 1H), 3.42 (dd, J = 12.4, 6.4 Hz, 1H), 1.58 (s, 3H), 1.53 (s, 3H), 1.47 (s, 3H), 1.29 (s, 3H)

Compound 36. A suspension of **35** (100 mg, 0.15 mmol) in acetone (1.0 mL) and water (0.3 mL) was treated with zinc (0.3 g) and ammonium chloride (0.3 g) at room temperature for 10 min. Organic layer was transferred to a new vial. The residue was extracted with acetone (1.0 mL), and the combined organic solution was evaporated. The residue was dissolved in methanol (1.0 mL) and then treated with HCl (2.0 mL, 2.0 N). The mixture was warmed to 60 °C for 10 min, and solvent was evaporated. The residue was treated with wet sodium bicarbonate and extracted with methanol (3 mL). Organic solution was evaporated, and the residue was used for next step.

Compound 14. To a solution of **36** in THF (2.0 mL) and triethyl amine (0.1 mL) was added chloroacetyl chloride (2.0 M solution in THF) at 0 °C, monitoring the reaction with HPLC until the starting material disappeared. 6-Mercaptonicotinic acid methyl ester (100 mg, 0.59 mmol) was introduced, and the resulting mixture was heated in a sealed tube at 100 °C for 5 min. Solvent was evaporated and the residue was purified using preparative HPLC to give the title compound **14** (45 mg, 39% two steps) as a yellow solid. MS (ES$^+$) m/z (M + 1) 775; ^{1}H NMR (400 MHz, DMSO) δ 9.62 (s, 1H), 9.13 (dd, J = 2.4, 0.8 Hz, 1H), 8.95 (d, J = 1.6 Hz, 1H), 8.33 (dd, J = 8.4, 2.4 Hz, 1H), 8.13 (dd, J = 8.4, 2.4 Hz, 1H), 8.03 (d, J = 8.4, Hz, 1H), 8.02 (s, 1H), 7.57 (d, J = 8.4 Hz, 1H), 7.30 (t, J = 1.6 Hz, 1H), 7.05 (dt, J = 10.0, 2.4 Hz, 1H), 6.88 (s, 1H), 6.56 (dt, J = 10.0, 2.4 Hz, 1H), 6.01 (t, J = 2.0 Hz, 1H), 4.89 (d, J = 6.0 Hz, 1H), 4.76 (d, J = 7.2 Hz, 1H), 4.42 (d, J = 7.2 Hz, 1H), 4.31 (d, J = 8.8 Hz, 1H), 4.15 (s, 2H), 4.12 (dd, J = 10.4, 6.0 Hz, 1H), 3.91 (s, 3H), 3.87 (s, 3H), 3.85 (s, 3H), 3.77 (t, J = 8.4 Hz, 3H), 3.72−3.67 (m, 2H), 3.52−3.47 (m, 1H), 3.10−3.04 (m, 1H).

Compound 9. A solution of **14** (95 mg, 12 mmol) in MeOH (0.5 mL) was treated with potassium carbonate (300 mg) and water (0.2 mL) in a capped vial at 80 °C for 5 min. Organic layer was transferred to a new vial, and then drops of formic acid were added. The pH was checked to ensure that the mixture is mildly acidic. The mixture was purified using preparative HPLC to give the title compound (38 mg, 42%) as a yellow solid. MS (ES$^+$) m/z (M + 1) 747; ^{1}H NMR(400 MHz, DMSO) δ 13.19 (br, 1H), 11.66 (s, 1H), 9.65 (s, 1H), 9.11 (dd, J = 2.4, 0.8 Hz, 1H), 8.94 (d, J = 1.2 Hz, 1H), 8.30 (dd, J = 6.0, 2.4 Hz, 1H), 8.10 (dd, J = 8.4, 2.4 Hz, 1H), 8.04 (s, 1H), 8.00 (dd, J = 8.4, 0.8 Hz, 1H), 7.54 (d, J = 8.4 Hz, 1H), 7.29 (t, 1.6 Hz, 1H), 7.04 (ddd, J = 9.6, 2.0, 1.2 Hz), 6.88 (s, 1H), 6.54 (ddd, J = 12.0, 2.4, 2.0 Hz, 1H), 5.99 (t, J = 4.8 Hz, 1H), 6.89 (d, J = 6.0 Hz, 1H), 4.76 (br, 1H), 4.41−4.25 (m, 3H), 4.13 (s, 2H), 4.11−4.09 (m, 1H), 3.84 (s, 3H), 3.82−3.65 (m, 4H), 3.52−3.47 (m, 1H), 3.10−3.03 (m, 1H).

Compound 37. A solution of 1-chloro-2-fluoro-4-methoxy-5-nitrobenzene (4.1 g, 20 mmol) (**19**) in DMSO (4.0 mL) was treated with potassium hydroxide (5.0 g) in water (5.0 mL). The mixture was heated slowly to 100 °C and then kept at this temperature for 1 h. The mixture was cooled to room temperature and diluted with DCM (50 mL) and then treated with $KHSO_4$ (excess). The organic solution was transferred, and the residue was washed with DCM (50 mL). The combined organic solution was dried and evaporated. The resulting solid was washed with water and a small amount DCM to give a yellow solid (3.5 g, 86%). ^{1}H NMR (400 MHz, CD_3Cl) δ 8.11 (s, 1H), 6.76 (s, 1H), 3.98 (s, 3H).

Compound 38. A mixture of **37** (5.89 g, 28.9 mmol), Zn (7.2 g), NH_4Cl (10 g), and water (13 mL) in 64 mL of acetone was stirred at room temperature for 30 min. After another 2 g of zinc was added, the mixture was stirred for another 15 min. The mixture was evaporated, and 250 mL of DCM was added. The mixture was stirred for 15 min and filtered. The residue was washed with EtOAc. The combined organics were dried, filtered, and evaporated to a dark brown solid (2.6 g, 52%).

Compound 39. A mixture of ethyl 6-chloro-3-pyridinecarboxylate (1.85 g, 10 mmol) and mercaptoacetic acid (1.2 g, 10 mmol) was heated without solvent at 100 °C for 10 min. The mixture was cooled to room temperature and washed with methanol (~10 mL) to give a white solid (2.1 g, 87%). ^{1}H NMR (400 MHz, $CDCl_3$) δ 13.06 (br, 1H), 8.24 (d, J = 2.0 Hz, 1H), 8.04 (dd, J = 9.6, 2.4 Hz, 1H), 6.60 (d, J = 9.6 Hz, 1H), 4.25 (q, J = 7.2 Hz, 2H), 1.38 (t, J = 7.2 Hz, 3H).

Compound 40. To a solution of the acid **39** (2.4 g, 9.95 mmol) and **38** (1.83 g, 10.5 mmol) in 70 mL of DMF were added DCC (2.63 g, 12.7 mmol) and HOBt (1.86 g, 13.8 mmol) at room temperature. The mixture was stirred at room temperature overnight and evaporated. The residue was worked up with DCM/saturated $NaHCO_3$ and chromatographed (EtOAc/heptane 1:3 to 1:1) to give a light brown solid (1.82 g, 46%). ^{1}H NMR ($CDCl_3$) (ppm) 9.66 (1H, s), 9.05 (1H, s), 8.35 (1H, s), 8.06 (dd, J = 6.2, 2.2 Hz, 1H), 7.27 (dd, J = 7.6, 0.8 Hz, 1H), 6.46 (1H, s), 4.36 (q, J = 7.1 Hz, 2H), 3.91 (2H, s), 3.71 (3H, s), 1.34 (t, J = 7.1 Hz, 3H).

Compound 41. Compound **25** (405 mg, 1.64 mmol) and K_2CO_3 (678 mg, 4.9 mmol) were suspended in 5 mL of anhydrous THF in a 25 mL round-bottom flask under Ar. The content was cooled to 0 °C, and then *tert*-butyl bromoacetate (955 mg, 2.0 mmol) was added in one portion. The reaction mixture was stirred at room temperature overnight. The solvent was removed on a rotavapor, and the residue was partitioned with EtOAc/water. The organic layer was separated, and

dx.doi.org/10.1021/jm3014844 | J. Med. Chem. XXXX, XXX, XXX−XXX

the aqueous layer was extracted with EtOAc once more. The combined organic layers were dried over anhydrous Na_2SO_4. The final product was purified by flash chromatography (EtOAc/hexanes) to give the final product as a thick oil (546 mg, yield 92%).

Compound 42. To compound **41** (314 mg, 0.87 mmol) in a 5 mL round-bottom flask was added TFA (1.3 mL). The solution was stirred at room temperature overnight. The solvent was removed in vacuo and the crude product was obtained (263 mg, 100%) as a white solid.

Compound 43. To a stirred solution of acid **42** (270 mg, 0.88 mmol), 3-amino 1-propanol (63 mg, 0.88 mmol), and HOBt (150 mg, 1.1 mmol) in DMF (9 mL) was added EDCI (300 mg, 1.49 mmol) in one portion at room temperature followed by addition of TEA (0.3 mL, 2.2 mmol), and the resultant mixture was stirred for overnight. Solvent was stripped under vacuum, and the residue was extracted with EtOAc (3 × 15 mL) and washed with 5% $NaHCO_3$ solution. The combined organic extracts were dried over Na_2SO_4 and concentrated in vacuo. The crude material was then flash-chromatographed over silica gel, eluting with hexane−EtOAc (2:8) to furnish the desired product (220 mg, 69%). ^{1}H NMR (DMSO-d_6, 400 MHz) δ 1.60 (m, 2H), 3.57 (m, 2H), 3.70 (s, 3H), 3.90 (m, 2H), 4.70 (s, 2H), 7.00 (m, 1H), 7.61 (m, 1H,), 7.75 (s, 1H) 8.15 (d, 1H, J = 8.8 Hz) 8.25 (m, 1H,) 8.40 (dd, 1H, J = 8.1, 2.0 Hz), 9.15 (dd, 1H, J = 2.0, 0.8 Hz). MS (ES+) m/z 362 (M + 1).

Compound 44. To a solution of triphenylphosphine (53 mg, 0.57 mmol) in THF (2.5 mL) was added DIAD (41 uL, 0.2 mmol) at 0 °C, and the mixture was stirred for 5 min. A mixture of the above compound **43** (73 mg, 0.2 mmol) and phenol **40** (80 mg, 0.2 mmol) were added together. The mixture was then stirred at room temperature overnight. Solvent was evaporated and the crude product was subjected to flash chromatography over silica gel, eluting with EtOAc to afford the product (50 mg, 33%). ^{1}H NMR (MeOD-d_4, 400 MHz) δ 1.40 (t, 3H), 1.91 (m, 2H), 3.55 (m, 2H), 3.70 (s, 3H), 3.90 (s, 2H), 3.91 (m, 2H), 4.33 (q, 2H), 4.70 (s, 2H), 6.80 (m, 1H), 7.33 (m, 1H,), 7.44 (m, 2H) 7.79 (d, 1H J = 9.2 Hz,) 8.00 (s, 1H,) 8.10 (dd, 1H, J = 8.1, 2.0 Hz), 8.25 (dd, 1H, J = 8.1, 2.0 Hz), 8.50 (s, 1H), 9.10 (dd, 2H, J = 1.6, 9.6 Hz). MS (ES+) m/z 740.17 (M + 1).

Compound 10. A solution of diester **44** (30 mg, 0.04 mmol) in MeOH (1.5 mL) was treated with potassium carbonate (200 mg) and water (0.6 mL) in a sealed microwave vial heated at 90 °C for 15 min. The mixture was sequestered with formic acid and directly injected on a preparative HPLC column, eluting with a mixture of ACN−H_2O with 0.1% HCO_2H to yield an off white solid (6 mg, 21%). ^{1}H NMR (MeOD-d_4, 400 MHz) δ 1.91 (m, 2H), 3.55 (m, 2H), 3.90 (s, 2H), 3.91 (m, 2H), 4.70 (s, 2H), 6.80 (m, 1H), 7.33 (m, 3H), 7.70 (d, 1H, J = 8.4 Hz) 8.15 (s, 1H), 8.20 (dd, 1H, J = 8.1, 2.0 Hz), 8.30 (m, 3H), 9.10 (dd, 2H, J = 1.2, 10.6 Hz). MS (ES+) m/z 698.12 (M + 1).

Compound 45. 2,3:4,5-di-*O*-Isopropylidenemannitol (**45**) was synthesized from 1,2:5,6-bis-*O*-(1-methylethylidene)-D-chiroinositol (6.5 g, 25 mmol) by utilizing the procedure as described for the synthesis of compound **29** in 70% yield as white solid.

Compound 46. A solution of 2,3:4,5-di-O-isopropylidenemannitol **45** (1.5 g, 5.7 mmol) in THF (30 mL) was treated with NaH (0.2 g, 5.0 mmol, 60% in mineral oil) at room temperature for 0.5 h. 2-Nitro-4-chloro-5-fluoroanisole (1.0 g, 4.9 mmol) was added, and the resulting mixture was warmed to 60 °C for 15 min. Solvent was evaporated and the residue was purified with a flash column chromatography (elution, DCM/MeOH = 100:0 to 5) to give the title compound (1.4 g, 64%) as a yellow solid.

^{1}H NMR (400 MHz, $CDCl_3$) δ 8.10 (s, 1H), 6.64 (s, 1H), 4.70 (ddd, J = 10.8, 6.4, 4.8 Hz, 1H), 4.56 (dd, J = 6.4, 4.4 Hz, 1H), 4.45−4.39 (m, 2H), 4.33 (dd, J = 11.6, 5.2 Hz, 1H), 4.21 (dd, J = 9.2, 4.4 Hz, 1H), 4.01 (s, 3H), 3.84−3.76 (m, 2H), 2.40 (br, 1H), 1.57 (s, 3H), 1.51 (s, 3H), 1.46 (s, 3H), 1.27 (s, 3H).

Compound 47. To a solution of triphenylphosphine (280 mg, 1.1 mmol) in DCM (3.0 mL) was added DIAD (135 uL, 0.69 mmol) at −20 °C, and the mixture was warmed to 0 °C for 10 min. A mixture of **46** (225 mg, 0.50 mmol) and **25** (125 mg, 0.50 mmol) was introduced. After 10 min at room temperature, the reaction vial was capped and heated at 60 °C for 10 min. Solvent was evaporated and the residue was purified with two preparative TLC plates (elution, DCM/AcOEt = 100:10) to give the title compound (237 mg, 70%) as a light yellow solid. ^{1}H NMR (400 MHz, DMSO) δ 9.14 (dd, J = 2.4, 0.8 Hz, 1H), 8.36 (dd, J = 8.0, 2.0 Hz, 1H), 8.18 (dd, J = 8.4, 0.8 Hz, 1H), 8.05 (s, 1H), 7.60−7.56 (m, 2H), 7.05 (ddd, J = 10.8, 2.4, 2.0 Hz, 1H), 7.02 (s, 1H), 4.66−4.61 (m, 2H), 4.67−4.46 (m, 3H), 4.34−4.27 (m, 2H), 4.15 (dd, J = 10.0, 6.4 Hz, 1H), 4.00 (s, 3H), 3.92 (s, 3H), 1.46 (s, 3H), 1.44 (s, 3H), 1.32 (s, 3H), 1.30 (s, 3H).

Compound 48. A suspension of **47** (450 mg, 0.66 mmol) in acetone (3.0 mL) and water (0.5 mL) was treated with zinc (3.0 g) and ammonium chloride (1.5 g) at room temperature for 10 min. Organic layer was transferred to a new vial. The residue was extracted with AcOEt (6.0 mL), and the combined organic solution was evaporated. The residue was dissolved in methanol (2.0 mL) and treated with HCl (4.0 mL, 2N) at 60 °C for 15 min. The solvent was evaporated to dry and the residue was dissolved in a mixture of THF (3.0 mL) and methanol (1.5 mL). The mixture was treated with wet sodium bicarbonate. After filtration, the organic solution was evaporated and the residue was used for next step.

Compound 49. To a solution of **48** in THF (3.0 mL) and triethylamine (0.3 mL) was added chloroacetyl chloride (2.0 M solution in THF) at −20 °C, monitoring the reaction with HPLC until the starting material disappeared. 6-Mercaptonicotinic acid methyl ester (200 mg, 1.2 mmol) was introduced. The resulting mixture was heated in a sealed tube at 100 °C for 5 min. Solvent was evaporated and the residue was purified with two preparative TLC plates (elution, DCM/MeOH/THF = 100:7:10) to give the title compound (160 mg, 31% three steps) as a white solid. MS (ES^+) m/z (M + 1) 776; ^{1}H NMR (400 MHz, DMSO) δ 9.62 (s, 1H), 9.17 (dd, J = 2.4, 0.8 Hz, 1H), 8.95 (d, J = 1.6 Hz, 1H), 8.36 (dd, J = 8.4, 2.4 Hz, 1H), 8.20 (dd, J = 8.4, 0.8 Hz, 1H), 8.13 (dd, J = 8.4, 2.4 Hz, 1H), 8.03 (s, 1H), 7.62 (d, J = 1.6 Hz, 1H), 7.58−7.54 (m, 2H), 6.97 (ddd, J = 10.8, 2.4, 2.0 Hz, 1H), 6.89 (s, 1H), 4.94 (d, J = 6.0 Hz, 2H), 4.91 (d, J = 6.0 Hz, 2H), 4.43 (d, J = 6.8 Hz, 2H), 4.42 (d, J = 6.8 Hz, 2H), 4.32 (m, 2H), 4.15 (s, 2H), 4.14−4.11 (m, 2H), 3.92 (s, 3H), 3.88 (s, 3H), 3.85 (s, 3H), 3.83−3.76 (m, 2H), 3.17 (d, J = 5.6, 1H).

Compound 50. To a solution of **36** in THF (2.0 mL) and triethylamine (0.1 mL) was added chloroacetyl chloride (2.0 M solution in THF) at 0 °C, monitoring the reaction with HPLC until the starting material disappeared. Mercaptopyridine (35 mg, 0.31 mmol) was introduced. The resulting mixture was heated in a sealed tube at 100 °C for 5 min. Solvent was evaporated. The residue was treated with aqueous sodium bicarbonate, and extraction was with DCM. Organic solution was evaporated, and the residue was used for next step.

Compound 12. A solution of **50** in methanol (0.5 mL) was treated with potassium carbonate (300 mg) and water (0.2 mL) in a capped vial at 80 °C for 5 min. Organic layer was transferred to a new vial, and then drops of formic acid were added. The pH was checked to ensure that the mixture is mildly acidic. The mixture was purified using preparative HPLC to give the title compound (11 mg, 10% from **36**) as a yellow solid. MS (ES^+) m/z (M + 1) 703; ^{1}H NMR (400 MHz, DMSO) δ 13.35 (br, 1H), 9.73 (s, 1H), 9.10 (d, J = 1.6 Hz, 1H), 8.52 (d, J = 4.0 Hz, 1H), 8.28 (dd, J = 8.4, 2.0 Hz, 1H), 8.10 (s, 1H), 7.97 (d, J = 8.0 Hz, 1H), 7.72 (td, J = 7.6, 2.0 Hz, 1H), 7.43 (d, J = 8.0 Hz, 1H), 7.29 (s, 1H), 7.22 (ddd, J = 7.2, 4.8, 0.8 Hz, 1H), 7.04 (dm, J = 10.0, 1H), 6.88 (s, 1H), 6.50 (dm, J = 11.6 Hz), 5.99 (t, J = 5.6 Hz, 1H), 4.90 (d, J = 5.6 Hz, 1H), 4.90 (d, J = 5.6 Hz, 1H), 4.77 (d, J = 4.4 Hz, 1H), 4.44 (d, J = 7.2 Hz, 1H), 4.37 (d, J = 7.2 Hz, 1H), 4.31 (d, J = 4.4 Hz, 1H), 4.12 (dd, J = 10.4, 6.4 Hz, 1H), 4.03 (s, 2H), 3.88 (m, 1H), 3.84 (s, 3H), 3.77 (t, J = 8.4 Hz, 1H), 3.69 (m, 1H), 3.55−3.47 (m, 1H), 3.10−3.04 (m, 1H).

Compound 53. To a solution of **30** (220 mg, 0.49 mmol) in DCM (3.0 mL) were added molecular sieves (0.5 g) and compound **52** (96 mg, 0.51 mmol). The resulting mixture was treated with $NaHB(OAc)_3$ (250 mg, 1.2 mmol) at room temperature for 2 h. Drops of water were added, and organic solution was transferred to a new vial. Solvent was evaporated and the residue was purified by using two preparative TLC plates (elution, DCM/MeOH = 100:3) to give the title compound (250 mg, 83%) as a yellow solid. ^{1}H NMR (400 MHz, $CDCl_3$) δ 8.71 (dt, J = 4.8, 0.8 Hz, 1H), 8.07 (s, 1H), 7.82 (dd, J = 8.0, 1.2 Hz, 1H), 7.71 (d, J = 8.0 Hz, 1H), 7.31 (td, J = 7.2, 0.8 Hz, 1H), 7.19 (s, 1H), 6.99 (ddd, J = 9.6, 2.0, 1.6 Hz, 1H), 6.63 (s, 1H), 6.42 (ddd, J = 10.8, 2.4, 2.0 Hz, 1H), 4.71−4.68 (m, 1H), 4.54−4.47 (m, 3H), 4.43 (dd, J = 9.6, 8.0 Hz, 1H),

dx.doi.org/10.1021/jm3014844 | J. Med. Chem. XXXX, XXX, XXX−XXX

4.20 (dd, J = 9.6, 4.4 Hz, 1H), 4.01 (m, 1H), 3.99 (s, 2H), 3.55 (dd, J = 12.4, 4.8 Hz, 1H), 3.42 (dd, J = 12.4, 7.2 Hz, 1H), 1.58 (s, 3H), 1.52 (s, 3H), 1.47 (s, 3H), 1.28 (s, 3H).

Compound 54. A mixture of **53** (350 mg, 0.57 mmol) in acetone (1.5 mL) was treated with zinc (0.5 g), ammonium chloride (0.3 g), and water (drops) at room temperature for 10 min. Organic solution was transferred to a new vial, and the residue was extracted with DCM (3.0 mL). The combined organic solution was dried and evaporated for the next step. The residue was dissolved in methanol (1.0 mL) and treated with HCl (2.0 mL, 2 N) at 60 °C for 15 min. The mixture was evaporated to dry, and the residue was dissolved in a mixture of THF (1.0 mL) and methanol (0.5 mL). The resulting solution was treated with wet sodium bicarbonate. After filtration, the organic solution was evaporated and the residue was for nest step.

Compound 55. To a solution of **54** in THF (2.0 mL) and triethylamine (0.05 mL) was added chloroacetyl chloride (2.0 M solution in THF) at 0 °C, monitoring the reaction with HPLC until the starting material disappeared. 6-Mercaptonicotinic acid methyl ester (120 mg, 0.71 mmol) was introduced. The resulting mixture was heated in a sealed tube at 100 °C for 5 min. Solvent was evaporated, and the residue was purified with a preparative TLC plate (elution, DCM/MeOH = 100:12) to give the title compound (110 mg, 27% from **53**) as an off white solid . ^{1}H NMR (400 MHz, DMSO) δ 9.63 (s, 1H), 8.96 (d, J = 1.6 Hz, 1H), 8.65 (dt, J = 4.4, 1.2 Hz, 1H), 8.14 (dd, J = 8.4, 2.4 Hz, 1H), 7.87 (dd, J = 4.4, 1.2 Hz, 1H), 7.58 (d, J = 8.4 Hz, 1H), 7.53 (m, 2H), 7.23 (t, J = 1.2 Hz, 1H), 6.98 (ddd, J = 10.4, 2.0, 1.2 Hz, 1H), 6.89 (s, 1H), 6.50 (dt, J = 12.0, 2.0 Hz, 1H), 5.91 (t, J = 5.6 Hz, 1H), 4.90 (d, J = 6.0 Hz, 1H), 4.76 (d, J = 6.0 Hz, 1H), 4.43 (d, J = 7.2 Hz, 1H), 4.37 (d, J = 7.6 Hz, 1H), 4.32 (dd, J = 10.4, 1.6 Hz, 1H), 4.16 (s, 2H), 4.13 (dd, J = 10.0, 2.0 Hz, 1H), 3.88 (s, 3H), 3.86 (s, 3H), 3.78 (t, J = 8.4 Hz, 1H), 3.74−3.65 (m, 2H), 3.50 (ddd, J = 12.8, 6.4, 2.4 Hz), 3.07 (ddd, J = 12.8, 7.2, 1.2 Hz, 1H).

Compound 13. A solution of **55** (90 mg, 0.13 mmol) in methanol (0.5 mL) was treated with potassium carbonate (300 mg) and water (0.2 mL) in a capped vial at 80 °C for 5 min. Organic layer was transferred to a new vial and diluted with DCM (2.0 mL) and then treated with drops of formic acid. The pH was checked to be pH 4−5. The yellow solid was collected by filtration and wash with water (1.5 mL), then DCM (1.0 mL). The dried solid was washed with a small amount of methanol to give the title compound (48 mg, 53%) as a yellow solid. MS (ES$^+$) m/z (M + 1) 703; ^{1}H NMR (400 MHz, DMSO) δ 9.66 (s, 1H), 8.94 (d, J = 1.2 Hz, 1H), 8.64 (ddd, J = 4.4, 1.6, 1.2 Hz, 1H), 8.11 (dd, J = 8.4, 2.0 Hz, 1H), 8.05 (s, 1H), 7.86 (d, J = 4.4 Hz, 1H), 7.85 (d, J = 4.8 Hz, 1H), 7.54 (d, J = 8.4 Hz, 1H), 7.34 (q, J = 4.4 Hz, 1H), 7.21 (t, J = 1.6 Hz, 1H), 6.97 (ddd, J = 9.6, 2.0, 1.6 Hz, 1H), 6.48 (ddd, J = 8.0, 2.4, 2.0 Hz, 1H), 5.90 (m, 1H), 4.89 (d, J = 2.0 Hz, 1H), 4.75 (d, J = 4.0 Hz, 1H), 4.42 (d, J = 6.4 Hz, 1H), 3.76 (d, J = 7.2 Hz, 1H), 4.31 (dd, J = 10.4, 2.0 Hz, 1H), 4.15 (s, 2H), 4.10 (d, J = 6.4 Hz, 1H), 3.87 (m, 1H), 3.85 (s, 3H), 3.79−3.04 (m, 4H), 3.51−3.47 (m, 1H), 3.07−3.03 (m, 1H).

Compound 51. A mixture of 2-bromopyridine (158 mg, 1.0 mmol), 3-(Cbz-amino)-5-fluorophenylboronic acid (289 mg, 1.0 mmol), K_3PO_4 (300 mg), $Pd_2(dba)_3$ (50 mg), 2-(dicyclohexylphosphino)biphenyl (38 mg), dioxane (2.0 mL), and water (1.0 mL) was degassed and then heated at 100 °C for 5 min. The reaction mixture was diluted with ethyl acetate (10 mL). Organic layer was separated and evaporated. The residue was purified by using two preparative TLC plates (elution, heptane/ethyl acetate = 3:1) to give the title compound (263 mg, 82%) as an off white solid. ^{1}H NMR (400 MHz, $CDCl_3$) δ 8.57 (ddd, J = 4.2, 2.0, 1.2 Hz, 1H), 7.65 (td, J = 8.0, 2.0 Hz, 1H), 7.60 (t, J = 1.6 Hz, 1H), 7.56 (d, J = 8.0 Hz, 1H), 7.36−7.23 (m, 7H), 7.15 (ddd, J = 7.2, 4.8, 0.8 Hz, 1H), 7.30 (br, 1H), 5.12 (s, 2H).

Compound 52. A solution of **51** (400 mg, 1.24 mmol) in methanol (10 mL) was charged with Pd−C (0.4 g) and hydrogenated under a hydrogen balloon at room temperature for 30 min. The catalyst was filtered off and the solvent evaporated to give the title compound (200 mg, 86%) as a brown solid. ^{1}H NMR (400 MHz, MeOD) δ 8.56 (ddd, J = 5.2, 2.0, 1.2 Hz, 1H), 8.12 (td, J = 8.0, 1.2 Hz, 1H), 7.72 (dt, J = 8.0, 1.2 Hz, 1H), 7.31 (ddd, J = 7.6, 4.8, 1.2 Hz, 1H), 7.05 (t, J = 2.0 Hz, 1H), 6.92 (ddd, J = 10.8, 2.4, 1.2 Hz, 1H), 6.50 (dt, J = 10.8, 2.0 Hz, 1H), 4.85 (s, 2H). Methanol (10 mL) was charged with Pd−C (0.4 g) and hydrogenated under a hydrogen balloon at room temperature.

■ ASSOCIATED CONTENT

Ⓢ Supporting Information

SPR sensograms, evaluation of reference compounds, and lactate assay reaction scheme. This material is available free of charge via the Internet at http://pubs.acs.org.

Accession Codes

The following X-ray crystal structures have been deposited in the RCSB Protein Data Bank: codes 4I8X, 4I9U, 4I9N, and 4I9H.

■ AUTHOR INFORMATION

Corresponding Author

*Phone: 617-621-2349. E-mail: anna.kohlmann@ariad.com.

Present Addresses

†Biogen Idec, 14 Cambridge Center, Cambridge, Massachusetts 02142, United States.

‡Belfer Institute, Dana Farber Cancer Institute, 77 Louis Pasteur Avenue, Boston, Massachusetts 02115, United States.

Notes

The authors declare no competing financial interest.

■ ACKNOWLEDGMENTS

The authors thank R. Anjum and V. Fantin for their work on target validation, M. Weigele for helpful discussions, L. Xue for assistance with analogue searches, and D. Myszka (Biosensor Tools, LLC) and A. Vinitsky (Affina Biotechnologies, Inc.) for providing SPR data and helpful discussions.

■ ABBREVIATIONS USED

LDH, lactate dehydrogenase; LDH-A, lactate dehydrogenase A; LDH-B, lactate dehydrogenase B; STD-NMR, saturation transfer difference NMR; SPR, surface plasmon resonance; CA-II, carbonic anhydrase II; CLM, common ligand mimic

■ REFERENCES

(1) Warburg, O. On respiratory impairment in cancer cells. *Science* **1956**, *124*, 269−270.

(2) Vander Heiden, M. G.; Cantley, L. C.; Thompson, C. B. Understanding the Warburg effect: the metabolic requirements of cell proliferation. *Science* **2009**, *324*, 1029−1033.

(3) Tennant, D. A.; Duran, R. V.; Gottlieb, E. Targeting metabolic transformation for cancer therapy. *Nat. Rev. Cancer* **2010**, *10*, 267−277.

(4) Warburg, O. On the origin of cancer cells. *Science* **1956**, *123*, 309−314.

(5) Ward, P. S.; Thompson, C. B. Metabolic reprogramming: a cancer hallmark even Warburg did not anticipate. *Cancer Cell* **2012**, *21*, 297−308.

(6) Hanahan, D.; Weinberg, R. A. Hallmarks of cancer: the next generation. *Cell* **2011**, *144*, 646−674.

(7) Eszes, C. M.; Sessions, R. B.; Clarke, A. R.; Moreton, K. M.; Holbrook, J. J. Removal of substrate inhibition in a lactate dehydrogenase from human muscle by a single residue change. *FEBS Lett.* **1996**, *399*, 193−197.

(8) Hewitt, C. O.; Eszes, C. M.; Sessions, R. B.; Moreton, K. M.; Dafforn, T. R.; Takei, J.; Dempsey, C. E.; Clarke, A. R.; Holbrook, J. J. A general method for relieving substrate inhibition in lactate dehydrogenases. *Protein Eng.* **1999**, *12*, 491−496.

(9) Read, J. A.; Winter, V. J.; Eszes, C. M.; Sessions, R. B.; Brady, R. L. Structural basis for altered activity of M- and H-isozyme forms of human lactate dehydrogenase. *Proteins* **2001**, *43*, 175−185.

(10) Goldman, R. D.; Kaplan, N. O.; Hall, T. C. Lactic dehydrogenase in human neoplastic tissues. *Cancer Res.* **1964**, *24*, 389−399.

(11) Giatromanolaki, A.; Sivridis, E.; Gatter, K. C.; Turley, H.; Harris, A. L.; Koukourakis, M. I. Lactate dehydrogenase 5 (LDH-5) expression in endometrial cancer relates to the activated VEGF/VEGFR2(KDR) pathway and prognosis. *Gynecol. Oncol.* **2006**, *103*, 912−918.
(12) Koukourakis, M. I.; Giatromanolaki, A.; Sivridis, E.; Gatter, K. C.; Harris, A. L. Lactate dehydrogenase 5 expression in operable colorectal cancer: strong association with survival and activated vascular endothelial growth factor pathway—a report of the tumour angiogenesis research group. *J. Clin. Oncol.* **2006**, *24*, 4301−4308.
(13) Lu, Y.; Liu, P.; Wen, W.; Grubbs, C. J.; Townsend, R. R.; Malone, J. P.; Lubet, R. A.; You, M. Cross-species comparison of orthologous gene expression in human bladder cancer and carcinogen-induced rodent models. *Am. J. Transl. Res.* **2011**, *3*, 8−27.
(14) Kolev, Y.; Uetake, H.; Takagi, Y.; Sugihara, K. Lactate dehydrogenase-5 (LDH-5) expression in human gastric cancer: association with hypoxia-inducible factor (HIF-1alpha) pathway, angiogenic factors production and poor prognosis. *Ann. Surg. Oncol.* **2008**, *15*, 2336−2344.
(15) Koukourakis, M. I.; Giatromanolaki, A.; Sivridis, E.; Bougioukas, G.; Didilis, V.; Gatter, K. C.; Harris, A. L. Lactate dehydrogenase-5 (LDH-5) overexpression in non-small-cell lung cancer tissues is linked to tumour hypoxia, angiogenic factor production and poor prognosis. *Br. J. Cancer* **2003**, *89*, 877−885.
(16) Deberardinis, R. J.; Sayed, N.; Ditsworth, D.; Thompson, C. B. Brick by brick: metabolism and tumor cell growth. *Curr. Opin. Genet. Dev.* **2008**, *18*, 54−61.
(17) Hsu, P. P.; Sabatini, D. M. Cancer cell metabolism: Warburg and beyond. *Cell* **2008**, *134*, 703−707.
(18) Kroemer, G.; Pouyssegur, J. Tumor cell metabolism: cancer's Achilles' heel. *Cancer Cell* **2008**, *13*, 472−482.
(19) Dang, C. V.; Semenza, G. L. Oncogenic alterations of metabolism. *Trends Biochem. Sci.* **1999**, *24*, 68−72.
(20) Le, A.; Cooper, C. R.; Gouw, A. M.; Dinavahi, R.; Maitra, A.; Deck, L. M.; Royer, R. E.; Vander Jagt, D. L.; Semenza, G. L.; Dang, C. V. Inhibition of lactate dehydrogenase A induces oxidative stress and inhibits tumor progression. *Proc. Natl. Acad. Sci. U.S.A.* **2010**, *107*, 2037−2042.
(21) Fantin, V. R.; St-Pierre, J.; Leder, P. Attenuation of LDH-A expression uncovers a link between glycolysis, mitochondrial physiology, and tumor maintenance. *Cancer Cell* **2006**, *9*, 425−434.
(22) Kanno, T.; Sudo, K.; Maekawa, M.; Nishimura, Y.; Ukita, M.; Fukutake, K. Lactate dehydrogenase M-subunit deficiency: a new type of hereditary exertional myopathy. *Clin. Chim. Acta* **1988**, *173*, 89−98.
(23) Rao, S. T.; Rossmann, M. G. Comparison of super-secondary structures in proteins. *J. Mol. Biol.* **1973**, *76*, 241−256.
(24) McClendon, S.; Vu, D. M.; Clinch, K.; Callender, R.; Dyer, R. B. Structural transformations in the dynamics of Michaelis complex formation in lactate dehydrogenase. *Biophys. J.* **2005**, *89*, L07−09.
(25) McClendon, S.; Zhadin, N.; Callender, R. The approach to the Michaelis complex in lactate dehydrogenase: the substrate binding pathway. *Biophys. J.* **2005**, *89*, 2024−2032.
(26) Choi, S. R.; Beeler, A. B.; Pradhan, A.; Watkins, E. B.; Rimoldi, J. M.; Tekwani, B.; Avery, M. A. Generation of oxamic acid libraries: antimalarials and inhibitors of *Plasmodium falciparum* lactate dehydrogenase. *J. Comb. Chem.* **2007**, *9*, 292−300.
(27) Choi, S. R.; Pradhan, A.; Hammond, N. L.; Chittiboyina, A. G.; Tekwani, B. L.; Avery, M. A. Design, synthesis, and biological evaluation of *Plasmodium falciparum* lactate dehydrogenase inhibitors. *J. Med. Chem.* **2007**, *50*, 3841−3850.
(28) Granchi, C.; Bertini, S.; Macchia, M.; Minutolo, F. Inhibitors of lactate dehydrogenase isoforms and their therapeutic potentials. *Curr. Med. Chem.* **2010**, *17*, 672−697.
(29) Ward, R. A.; Brassington, C.; Breeze, A. L.; Caputo, A.; Critchlow, S.; Davies, G.; Goodwin, L.; Hassall, G.; Greenwood, R.; Holdgate, G. A.; Mrosek, M.; Norman, R. A.; Pearson, S.; Tart, J.; Tucker, J. A.; Vogtherr, M.; Whittaker, D.; Wingfield, J.; Winter, J.; Hudson, K. Design and synthesis of novel lactate dehydrogenase A inhibitors by fragment-based lead generation. *J. Med. Chem.* **2012**, *55*, 3285−3306.
(30) Irwin, J. J.; Sterling, T.; Mysinger, M. M.; Bolstad, E. S.; Coleman, R. G. ZINC: a free tool to discover chemistry for biology. *J. Chem. Inf. Model.* **2012**, *52*, 1757−1768.
(31) Congreve, M.; Carr, R.; Murray, C.; Jhoti, H. A "rule of three" for fragment-based lead discovery? *Drug Discovery Today* **2003**, *8*, 876−877.
(32) Mayer, M.; Meyer, B. Characterization of ligand binding by saturation transfer difference NMR spectroscopy. *Angew. Chem., Int. Ed.* **1999**, *38*, 1784−1788.
(33) Neumann, T.; Junker, H. D.; Schmidt, K.; Sekul, R. SPR-based fragment screening: advantages and applications. *Curr. Top. Med. Chem.* **2007**, *7*, 1630−1642.
(34) Sass, C.; Briand, M.; Benslimane, S.; Renaud, M.; Briand, Y. Characterization of rabbit lactate dehydrogenase-M and lactate dehydrogenase-H cDNAs. Control of lactate dehydrogenase expression in rabbit muscle. *J. Biol. Chem.* **1989**, *264*, 4076−4081.
(35) Halgren, T. New method for fast and accurate binding-site identification and analysis. *Chem. Biol. Drug Des.* **2007**, *69*, 146−148.
(36) Halgren, T. A. Identifying and characterizing binding sites and assessing druggability. *J. Chem. Inf. Model.* **2009**, *49*, 377−389.
(37) Abel, R.; Young, T.; Farid, R.; Berne, B. J.; Friesner, R. A. Role of the active-site solvent in the thermodynamics of factor Xa ligand binding. *J. Am. Chem. Soc.* **2008**, *130*, 2817−2831.
(38) Cameron, A.; Read, J.; Tranter, R.; Winter, V. J.; Sessions, R. B.; Brady, R. L.; Vivas, L.; Easton, A.; Kendrick, H.; Croft, S. L.; Barros, D.; Lavandera, J. L.; Martin, J. J.; Risco, F.; Garcia-Ochoa, S.; Gamo, F. J.; Sanz, L.; Leon, L.; Ruiz, J. R.; Gabarro, R.; Mallo, A.; Gomez de las Heras, F. Identification and activity of a series of azole-based compounds with lactate dehydrogenase-directed anti-malarial activity. *J. Biol. Chem.* **2004**, *279*, 31429−31439.
(39) Conners, R.; Schambach, F.; Read, J.; Cameron, A.; Sessions, R. B.; Vivas, L.; Easton, A.; Croft, S. L.; Brady, R. L. Mapping the binding site for gossypol-like inhibitors of *Plasmodium falciparum* lactate dehydrogenase. *Mol. Biochem. Parasitol.* **2005**, *142*, 137−148.
(40) Kuntz, K.; Uehling, D. E.; Waterson, A. G.; Emmitte, K. A.; Stevens, K.; Shotwell, J. B.; Smith, S. C.; Nailor, K. E.; Salovich, J. M.; Wilson, B. J.; Cheung, M.; Mook, R. A.; Baum, E. W.; Moorthy, G. US 2008300242 A1, 2008; 249 pp; Glaxosmithkline LLC.
(41) Mueller, R.; Yang, J.; Duan, C.; Pop, E.; Zhang, L. H.; Huang, T. B.; Denisenko, A.; Denisko, O. V.; Oniciu, D. C.; Bisgaier, C. L.; Pape, M. E.; Freiman, C. D.; Goetz, B.; Cramer, C. T.; Hopson, K. L.; Dasseux, J. L. Long hydrocarbon chain ether diols and ether diacids that favorably alter lipid disorders in vivo. *J. Med. Chem.* **2004**, *47*, 5183−5197.
(42) Sem, D. S.; Bertolaet, B.; Baker, B.; Chang, E.; Costache, A. D.; Coutts, S.; Dong, Q.; Hansen, M.; Hong, V.; Huang, X.; Jack, R. M.; Kho, R.; Lang, H.; Ma, C. T.; Meininger, D.; Pellecchia, M.; Pierre, F.; Villar, H.; Yu, L. Systems-based design of bi-ligand inhibitors of oxidoreductases: filling the chemical proteomic toolbox. *Chem. Biol.* **2004**, *11*, 185−194.
(43) Ferreira, R. S.; Bryant, C.; Ang, K. K.; McKerrow, J. H.; Shoichet, B. K.; Renslo, A. R. Divergent modes of enzyme inhibition in a homologous structure−activity series. *J. Med. Chem.* **2009**, *52*, 5005−5008.
(44) Giannetti, A. M.; Koch, B. D.; Browner, M. F. Surface plasmon resonance based assay for the detection and characterization of promiscuous inhibitors. *J. Med. Chem.* **2008**, *51*, 574−580.
(45) Abel, R.; Salam, N.; Beuming, T.; Sherman, W.; Farid, R. Presented at the National Meeting of the American Chemical Society, 2010; COMP-79.
(46) *Glide*, version 5.5; Schrodinger, LLC.: New York, NY, 2009.
(47) *Ligprep*, version 2.3; Schrodinger, LLC.: New York, NY, 2009.
(48) *Prime*, version 2.1; Schrodinger, LLC.: New York, NY, 2009.